Chapter 2

Iron-based Nanomaterials in the Catalysis

Boris I. Kharisov, Oxana V. Kharissova, H.V. Rasika Dias,
Ubaldo Ortiz Méndez, Idalia Gómez de la Fuente, Yolanda Peña and
Alejandro Vázquez Dimas

Additional information is available at the end of the chapter

http://dx.doi.org/10.5772/61862

Abstract

Available data on catalytic applications of the iron-containing nanomaterials are reviewed. Main synthesis methods of nZVI, nano-sized iron oxides and hydroxides, core-shell and alloy structures, ferrites, iron-containing supported forms, and composites are described. Supported structures include those coated and on the basis of polymers or inert inorganic materials (*i.e.*, carbon, titania or silica). Description of catalytic processes includes the decomposition reactions (in particular photocatalytic processes), reactions of dehydrogenation, oxidation, alkylation, C–C coupling, among a series of other processes. Certain attention is paid to magnetic recovery of catalysts from reaction systems and their reuse up to several runs almost without loss of catalytic activity.

Keywords: Iron nanomaterials, ferrites, catalysis, bimetallic nanoparticles, core-shell nanoparticles

1. Introduction

1.1. General information on the iron-containing nanostructures

Nanomaterials on iron basis mainly include zero-valent iron (ZVI and nZVI (nano zero-valent iron) are nowadays classic terms), iron-based nanoalloys or core-shell nanoparticles, iron(II and III) oxides, and ferrites, among others. Metallic iron is normally covered with iron(II) and iron(III) oxides [1]. The iron oxides (iron oxide nanoparticles are also referred in several reports to as superparamagnetic iron-oxide nanoparticles (SPIONs) although SPIONS have inducible

magnetic properties) [2, 3], belong to the most technologically important oxides of transition metals. The collective term "iron oxides" is also used for oxides, hydroxides, and oxy-hydroxides containing Fe(II) and/or Fe(III) cations and OH^- and/or O^{2-} anions. In total, sixteen pure iron oxide phases, *i.e.,* oxides, hydroxides or oxy-hydroxides, are currently known. These compounds are $Fe(OH)_3$, $Fe(OH)_2$, $Fe_5HO_8 \cdot 4H_2O$, Fe_3O_4, FeO, five polymorphs of FeOOH and four of Fe_2O_3. In these oxide compounds, which are generally low soluble and possess brilliant colors, the iron is present in the form of Fe(III). The extremely important advantages of nanostructured iron, in comparison with other nanomaterials, are its relatively low toxicity and capacity to be biodegradable. This metal, in addition, is non-expensive and commonly widespread material [4].

Particle diameters of nZVI are normally in the range from 10 to 100 nm [5], exhibiting a classic core-shell structure. Their core contains metallic iron phase, meanwhile the oxidation products of zero-valent iron form mixed valent [*i.e.,* Fe(II) and Fe(III)] oxide shell. If stabilizers in excess are present, these core-shell nanoparticles could be protected against further oxidation [6]. Among such stabilizers, a series of organic compounds can be used for nZVI functionalization to stabilize nZVI aqueous dispersions, inhibiting strongly their further agglomeration. Such compounds can be used to satisfy this purpose, for example, PEG, polyacrylic acid, 4-butane-diphosphonic acid, and methoxyethoxyethoxyacetic acid (MEEA) [7].

The magnetite (Fe_3O_4) and maghemite (γ-Fe_2O_3) are of a particular interest talking about iron oxides (SPIONs). The magnetite structure corresponds to an inverse spinel ferrite. The oxygen ions are the part of a close-packed cubic lattice, containing the iron ions between two different interstices, tetrahedral sites (A), and octahedral sites (B). In a chemical point of view, the magnetite/maghemite can be represented by the following formula: Fe^{3+} $[Fe^{2+}_{1-y}$ Fe^{3+}_{1-y} $Fe^{3+}_{1.67y}\square_{0.33y}]O_4$, where y=0 for pure magnetite and y=1 for pure maghemite (completely oxidized magnetite). From room temperature up to Curie temperature (T_c=860 K), the A sites are filled by Fe^{3+} ions and the B sites are filled by Fe^{3+} and Fe^{2+} ions in equal quantity. Although the lepidocrocite (γ-FeOOH) dehydration transforms into γ-Fe_2O_3, industrial fabrication of maghemite is based on a multistep process (1):

$$\begin{aligned}&(\alpha \text{ and/ or } \gamma)\text{-FeOOH}(\text{oxidation}) \rightarrow \alpha\text{-Fe}_2\text{O}_3(\text{reduction}) \rightarrow \\ &\rightarrow \text{Fe}_3\text{O}_4(\text{controlled oxidation}) \rightarrow \gamma\text{-Fe}_2\text{O}_3\end{aligned} \tag{1}$$

In addition to the nZVI and SPIONs, a variety of composite inorganic iron-based nanomaterials have been discovered, in particular core-shell Fe(or Fe_xO_y)/Au or more complex trimetallic nanoparticles such as $(Fe_{60}Co_{49})_{core}/Au_{shell}$ [8]. These nanoparticles were classified [9] on the basis of on their complexity levels: 1) the nanostructures based of an iron-containing material with magnetic properties *different from iron oxide*; 2) the nanostructures with a non-spherical morphology (*e.g.* hollow structure); 3) the nanostructures with multi-material composition, *i.e.* each of them is constructed ≥2 more domains of joined together different inorganic materials.

2. Main synthesis methods

A number of currently used methods, shown below, are nowadays used for preparation of Fe-containing nanomaterials. At the same time, some well-known conventional *wet chemistry routes* have not been forgotten and are applied for nZVI synthesis [10] (for instance, by a borohydride reduction in laboratory scale) [11], Fe_2O_3 (sol-gel technique [12] or electrochemical deposition [13]), or Fe_3O_4 (urea- and NaOH-assisted hydrolysis of Fe^{3+} and Fe^{2+} salts and further *ultrasonic treatment* of $FeO(OH)/Fe(OH)_2$). Particle sizes and morphologies of the formed nanomaterials, synthesized by distinct methods, can vary depending on the synthesis conditions. For example, the Fe_3O_4 nanoparticles [14], obtained by *radio frequency nitrogen plasma* technique, represent a regular spherical form, meanwhile the nanoparticles synthesized by wet chemistry synthesis were seen as well shaped cubic form. In case of the plasma prepared iron oxides, their size distribution was wider resulting small (25–80 nm) and larger (>100 nm) particles.

2.1. nZVI and Fe-M nanoalloys and core-shell nanostructures

To produce nanopowders, the method of *electrical explosion of wire* was applied [15, 16], among other physical methods. Intermetallic phases can also be obtained by the *arc discharge* technique, for example Fe-Sn bimetallic nanoparticles [17]. Thus prepared nanoparticles have a core/shell structure consisting of a SnO_2 shell (5–10 nm in thickness) and a core containing polycrystalline intermetallic compounds. The intermetallic compounds $FeSn_2$ and Fe_3Sn_2 were shown to be generated; they coexist with the Sn phase as a single nanoparticle. *Microwave irradiation* (which is used to fabricate normally inorganic materials and composites, lesser organic- or organometallic-based materials), is an alternative method in comparison with classic heating of product precursors. Metal transformations in microwave field are extensively reviewed in a comprehensive recent book [18]. Elemental metal nanoparticles in various forms can also be fabricated using this method. For example, iron-based nanoparticles were obtained applying microwave–polyol route in ethyleneglycol at 100 and 150 °C with additives of polyvinyl pyrrolidone and dodecyl amine [19]. Also, pulsed excimer *laser radiation* (248 nm) was used to ablate a feedstock of permalloy (~2 μm, Ni 81%:Fe 19%) under both normal atmospheric conditions (in air) and in other gases, as well as under pressures [20]. α-Fe nanoparticles were also obtained with use of a modified *metal-membrane incorporation* method applying diffusing metal ions through a dialysis membrane [21] (the diffusion-time ≤15 min).

To get nZVI in laboratory conditions [22], the classic and usual synthesis technique is the reduction of Fe(II or III) salts using $NaBH_4$, $NaAlH_4$ or $LiAlH_4$ as reductants. Thus, nZVI was synthesized (reaction 2) [23] in ethanol medium by the method of reduction of FeX_n (X= Cl, OH, OR, CN, OCN, SCN) using sodium borohydride under atmospheric conditions [24].

$$2\,FeCl_3 + 6\,NaBH_4 + 18\,H_2O \rightarrow 2\,Fe^0 + 6\,NaCl + 6\,B(OH)_3 + 21\,H_2 \qquad (2)$$

A patent [25] describes a route to metal nanoparticles by *thermal decomposition* of iron acetate $Fe(OOCCH_3)_2$, placed in a reaction vessel with a passivating solvent such as a glycol ether. Discussing the *pyrolysis* method, it should be noted the preparation of iron nanoparticles (embedded in a carbon matrix) from metal phthalocyanine as precursor [26] and carbon-encapsulated iron nanoparticles (size 5–20 nm) *via* a picric acid-*detonation-induced pyrolysis* of ferrocene as precursor; this route has such peculiarities as self-heating and extremely fast process [27]. Also, the *"greener" techniques* [28, 29, 30, 31, 32] have been applied for nanoparticle fabrication. Use of plant extracts and other natural products on polyphenole basis in these syntheses as reductants and capping agents at the same time for obtaining nZVI and several other Fe-containing nanoparticles is intriguing [33] as well. For instance, the *herbal tea extracts* were applied to reduce iron(III) chloride to elemental iron nanoparticles (50 nm) [34].

In addition, a variety of general physico-chemical methods have been applied for the production of as *Fe-containing bi- and polymetallic alloys* as core-shell nanostructures. For instance, high entropy Nd-Fe-Co-Ni-Mn alloy nanofilms were prepared [35] by *electrodeposition* at r.t. After preliminary preparation of alumina nanotemplates, Fe, Fe-Ni, and Fe-Pd nanowires were successfully electrodeposited within their porous structure. Also, the Fe-Pt nanocrystalline magnetic films (200 nm of thickness) with planar texture were obtained with use of *magnetron sputtering* and crystalline annealing in magnetic field [36].

2.2. Supported and coated iron nanoparticles

A number of publications are devoted to *carbon-supported* ZVI nanomaterials [37]. This type of protective carbon-cage encapsulation of iron nanoparticles can result hybrid core-shell nanomaterials with unique properties [38]. This way, carbon encapsulated iron core-shell nanoparticles (15–40 nm in size) were obtained *via* confined *arc plasma method* [39]. Resulting nanoparticles possessed a clear core-shell structure. The core (16 nm in diameter) of the particles corresponded to a BCC iron structure, and the shell (thickness 6–8 nm) was shown to be disorder carbon phase. A closely related *arc discharge technique* [40] is also frequently used for obtaining a variety of nanomaterials, in particular the iron containing ones. For instance, a simple, inexpensive and one-step arc discharge synthesis technique to prepare metal-containing carbon nanocapsules in aqueous solution is known [41]. It was established that iron nanoparticles can be *in situ* encapsulated in carbon shells when the arc discharge process was carried out in aqueous solutions of $FeSO_4$.

Combustion synthesis of iron oxide/iron-coated carbons such as cellulose fiber, anthracite, and activated carbon was reported a classic microwave oven with inverter technology [42]. The size of the iron oxide/iron nanoparticle-coated samples were determined to be in the range of 50–400 nm. It was found that iron oxide/iron nanoparticles exist in 4 main phases: γ-Fe_2O_3, α-Fe_2O_3, Fe_3O_4, and Fe, some of them had significant arsenic adsorption. In addition, carbon-coated iron nanoparticles with well-developed quasi-spherical shape were prepared with $Fe(NO_3)_3 \cdot 9H_2O$ and starch as carbon source [43, 44]. This is an efficient approach for the mass production of nanocage structures under mild conditions, which needs to be further explored for preparing various carbon coated metal nanomaterials. *Radiation methods* are being applied more widely last 10–15 years, in that case for preparation of Fe-carbon-supported nanostruc-

tures. This way, 2 types of amorphous carbon films (15 at.% iron containing film) were deposited onto Si substrates by a sputtering method and further exposed to an electron flow, where the energy and dose rate were much smaller compared to the electron beam in a TEM. In this case, graphitic structures were observed in amorphous matrix at temperatures up to 450 K. It was established that the graphitization progressed more intensively during the electron irradiation than in annealing at 773 K. This was attributed to thermal and catalytic effects, strongly related to grain growth of metal clusters.

2.3. Free and supported iron oxides and ferrites

Zeolites and closely related supporting materials represent an ideal basis for iron oxide nanocomposites. This way, the zeolite loading with nanoiron oxide by a simple chemical process was described [45]. Final crystallite sizes of the doped nanomaterials were in the range of 4–6 nm. It was shown that the zeolites become to have magnetic properties after being doped with nanoiron oxide. Mesoporous nanocomposites "iron oxide/silicate" Fe_2O_3-SBA-15 (SBA-15 is an abbreviation for hexagonally ordered mesoporous silica) with iron loadings of 1.2–35.8 wt.% were prepared hydrothermally [46]. It was revealed that these composites contain well-dispersed iron oxide nanoclusters in the walls of ordered mesoporous silica and high surface area. Certain number of composite nanomaterials based on Fe_3O_4 is known, for instance core/shell Fe_3O_4 coated gold nanoparticles (diameter 50–100 nm) [47]. Their possible formation mechanism was proposed as follows: pH-sensitive polymer owing to a shrunken or stretched structure of polyethyleneimine (PEI), led to the aggregation of the Fe_3O_4-gold seed nanoparticles, then gold reduces onto the surface of Fe_3O_4-gold seed nanoparticles. It was concluded that these core/shell multifunction nanomaterials will not only have external magnetic separation by the core of Fe_3O_4 but also detect the large biological molecules using the shell of gold. In addition, iron phthalocyanine prepolymer/Fe_3O_4 nano hybrid magnetic material [48] can be applied as high temperature-resistant polymer magnetic composite material. At last, ferrites having different sizes, from ultrasmall (2 nm) to 50 nm, can be fabricated by distinct techniques [49] mainly co-precipitation method (CPM), sometimes without using any capping agents/surfactants.

3. Catalytic applications

3.1. nZVI and supported Fe^0 nanocomposites

3.1.1. Catalyzed removal or decomposition of pollutants

nZVI has been extensively reported to resolve a series of environmental problems, related with destruction, adsorption, precipitation, reduction or oxidation of heavy metals, salt anions, hydrocarbons and halogenated organic pollutants (Fig. 1) [50], leading to their conversion to final non-hazardous products. In these processes, iron nanoparticles have shown high efficiency and practically no damage for the environment because of absence of toxicity. Thus, the efficiencies of *nitrate removal* from aqueous solution by single (TiO_2 and nZVI), and

composite (nano-TiO_2–Fe^0 composite, NTFC) system under UV illumination were studied [51]. Among the three systems, both nZVI and NTFC can effectively remove nitrate. However, only NTFC can achieve satisfactory transformation of nitrate to N_2. Reactive materials for catalytic *degradation of chlorinated organic compounds* in water at ambient conditions have been prepared on the basis of silica-supported Pd-Fe nanoparticles [52]. Nanoscale Fe-Pd particles were synthesized inside porous silica supports using $(NH_4)_3[Fe(C_2O_4)_3]$ and $[Pd(NH_3)_4]Cl_2$ or Pd acetate as reaction precursors. The reduction of these supported precursors using hydrogen led to materials, revealed high activity in the processes of perchloroethene (PCE) degradation and 2-chlorobiphenyl (2-ClBP) dechlorination. It was established that highly dispersed amorphous Fe-Pd bimetallic nanoparticles on silica support possess superior catalytic activity against PCE dechlorination, comparing with the free-standing Fe-Pd nanoparticles. It was also established that the addition of vitamin B12 (it is known to be an effective electron mediator, having strong synergistic effects with nZVI for reductive dehalogenation reactions) can significantly enhance the reductive dechlorination of PCE by nZVI [53]. A remarkable reductive dechlorination of PCE (0.25±0.01 h^{-1}) was observed in nZVI suspension (0.05 g/24 mL) with 0.5 mM vitamin B12 in 6 h, while no significant reductive dechlorination of PCE was observed in the nZVI suspension without vitamin B12. Similar composite material based on deposition of nZVI particles and cyanocobalamine (vitamin B12) on a diatomite matrix was also used for catalytic transformation of PCE and other organic contaminants in water [54]. The composite material rapidly degrades or transforms completely a large spectrum of water contaminants, including halogenated solvents like TCE, PCE, and *cis*-DCE, pesticides like alachlor, atrazine and bromacyl, and common ions like nitrate, within minutes to hours. In a related publication [55], iron nanoparticles were applied for remediation of PCB-contaminated soil, taking into account a maximization of PCB destruction in each treatment stage. The efficiency of PCB destruction during the first step treatment (mixing of soil and iron nanoparticles in water) can be improved by increasing the water temperature. The PCB destruction efficiency of minimum 95% can be achieved. In air at 300 °C, Fe_2O_3 is also a good catalyst for remediating PCB-contaminated soils. In addition, photo-Fenton like method using nZVI/UV/H_2O_2 was applied [56] for removing total *petroleum hydrocarbons* (TPH) and determining the optimal conditions using Taguchi method. The removal rate in optimal conditions was between 95% and 100%. The nZVI particles can be reused in a magnetic field. This process may enhance the rate of diesel degradation in polluted water and could be used as a pretreatment step for the biological removal of TPH from diesel fuel in the aqueous phase. Among other degradation applications, we note the use of nZVI/AC for catalytic wet peroxide oxidation of phenol [57]. The catalytic activity of phenol degradation was improved by application of nZVI/AC catalysts compared to that of Fe/AC. For the range 150–1,000 mg/L, the phenol conversion ≥90% can be achieved using these nanocatalysts during 15 min of the reaction in presence of the stoichiometric hydrogen peroxide for complete mineralization. At last, as an example of classic organic synthesis, we emphasize the conversion of synthesis gas to C2 through C4 olefins with up to 60% selectivity by carbon [58], using catalysts which comprise Fe promoted nanoparticles (5–30 nm in diameter) homogeneously dispersed on weakly interactive α-alumina or carbon nanofiber supports.

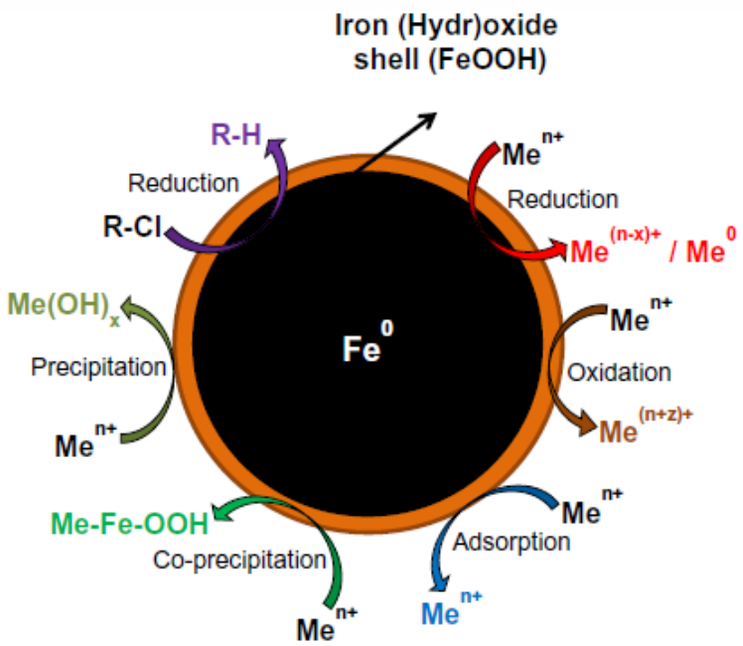

Figure 1. Core–shell structure of nZVI depicting various mechanisms for the removal of metals and chlorinated compounds. Adapted from Li et al. 2006 with permission.

Degradation of dyes with use of nZVI is carried out mainly on carbon-based nanocomposites. Thus, nZVI/activated carbon (nZVI/AC) was investigated as heterogeneous Fenton catalyst in 3D electrode system for methyl orange (MO) degradation [59]. The mineralization of MO was significantly improved by 20–35% compared to 2D AC system at the optimum conditions. A possible mechanism for decolorization and mineralization was proposed, which was attributed to the combination of adsorption, anodic oxidation, and Fenton oxidation in 3D nZVI/AC system. As an example of application of CNTs-based system, an ozone catalyst capable of working on acidic solution environments (labeled as CNTs-Fe^0), which was prepared by immobilizing nZVI onto the surface of MWCNTs and used for decomposition of methylene blue (MB) by formed hydroxyl radicals (HO·) [60]. At pH 3, the production of HO· was found to be considerably accelerated in the presence of CNTs-Fe^0 about 80 times in comparison with results using plain ozone. In the process of CNTs-Fe^0 catalytic ozonation, the CNTs support was analyzed to perform as effective "promoter" allowing the fast surface-mediated reactions, owing to the combination of its surface-active nature, conductivity, and chemical stability. All these and above technologies perfectly fit into advanced water treatment technologies, whose additional representative example is as follows. Thus, the *in situ* synthesis of air-stable nZVI embedded in cellulose fibers led to the assembly of highly reactive magnetic filter papers (membrane nanocomposites) [61]. This nZVI@FP nanocomposite (Fig. 2) showed high activity towards the removal of hexavalent chromium as well as an excellent catalytic ability to convert phenols into catechols, by simple filtration processes of the contaminated water solutions.

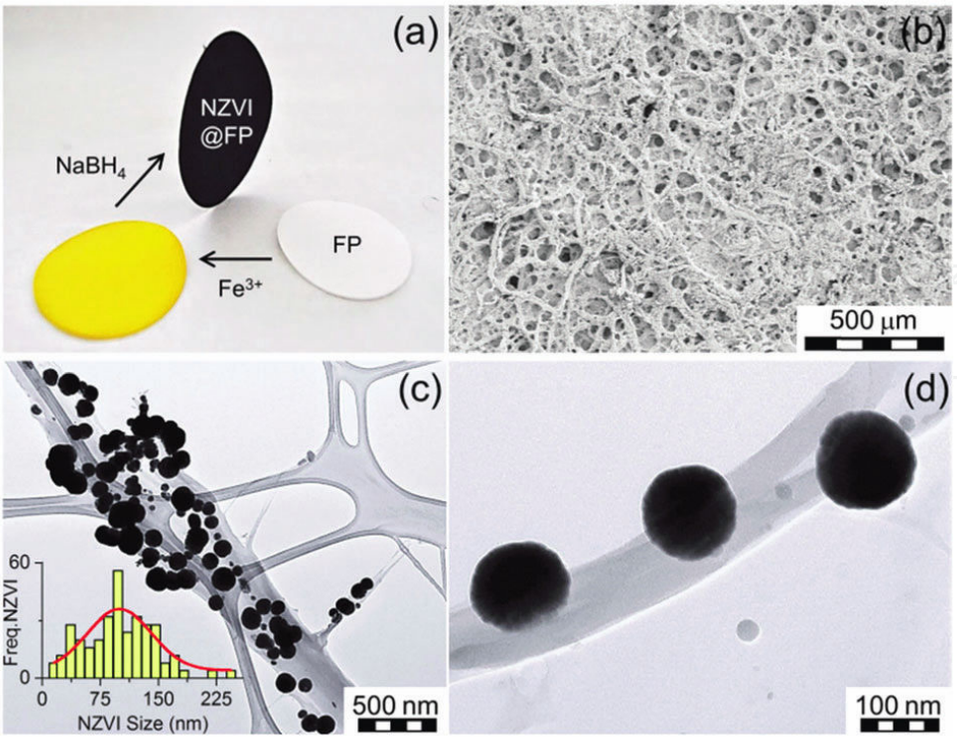

Figure 2. (a) Optical image showing the 2-step assembly of the magnetic nZVI@FP nanocomposite. (b) Scanning electron micrograph of nZVI@FP loaded with 5% in weight of nZVI. (c) TEM micrograph of NZVI entrapped over a cellulose fibre of FP. The inset shows the particle size distribution, as estimated from TEM (Freq.-nZVI *vs*. nZVI-size), together with the fitting analysis (red-line). (d) TEM micrograph of a magnified region of (c) revealing the intimate interaction between NZVIs and the fiber surface. FP = filter paper. Adapted from Datta et. al. 2014 with permission.

3.2. Fe–M nanoalloys, bimetallic NPs and core–shell nanostructures

Degradation of pollutants. Iron-based alloys, core-shell, and bimetallic nanoparticles, especially with noble metals, have been extensively applied in the catalysis and reviewed [62, 63, 64], so we will present in this section only their most representative recently reported examples. As well as nZVI described above, bimetallic Fe-containing nanoparticles (Fe with Pt, Ru, Rh, Ni, Co, Au, Cu, Ag) are used for the catalytic elimination of environmental pollutants. Reactions between them (pollutants and nanoparticles) can be mainly divided in 4 types [65]: a) catalytic replacement reactions for removal of heavy metals, b) hydrodehalogenation reactions (in case of halogenated hydrocarbons), c) azo and nitro hydrogenation reactions (for azo and nitro) compounds, and d) hydrodeoxygenation reactions (for oxyanions). In comparison with monometallic iron nanoparticles, the bimetallic iron NPs have considerable capacity to be separated and catalytic ability for degradation of non-biodegradable pollutants. Among them, Fe-Pt NPs are of an especial interest. Thus, Pt-Fe application as heterogeneous Fenton-like catalysts was reported for hydrogen peroxide decomposition and the decolorization of methylene blue [66]. FePt (and also Fe_3O_4, see more information below) NPs were prepared and tested as heterogeneous Fenton-like catalysts to evaluate and compare their efficiency toward the decolorization of MB dye in solution. Both FePt and Fe_3O_4 exhibited high activity toward the MB decolorization reaction though FePt exhibited a reaction rate that

was 100 times faster for a 5 ppm catalyst concentration. Both FePt and Fe_3O_4 NPs are superparamagnetic and thus can be easily separated with a magnet and reused for subsequent catalytic cycles. The same objective was reached using core-shell NPs on the nZVI basis. Thus, a series of nanocomposites consisting of nZVI encapsulated in SiO_2 microspheres were applied for the degradation of organic dyes was investigated using MB as the model dye in the presence of H_2O_2 [67]. The degradation efficiency and apparent rate constant of the degradation reaction were significantly enhanced with increased nZVI encapsulated in SiO_2 microspheres, whereas the dosage of H_2O_2 remarkably promoted degradation rate without affecting degradation efficiency.

It should be also noted that Fe-containing *thin films* can be applied for dye degradation. Thus, 2D nano-TiO_2 and Fe-doped nano-TiO_2 thin films with large sizes were obtained [68] at low temperature in an aqueous system via molecular self-assembly approach. Degradation of methyl orange solution under action of UV and visible light radiation was applied for evaluation of the photocatalytic activity. The doped iron presence was shown to improve the TiO_2 photocatalytic activity. The degradation yields of methyl orange were 98.62% and 89.24%, respectively, under illumination by UV lamp and using visible light. As an example of another degradation process, we note that the longevity and reactivity of nZVI and palladized bimetallic particles (BNP) were evaluated in batch and column experiments for remediation of a trichloroethene (TCE)-contaminated plume within a clayey soil [69]. The particle behavior was found to be severely affected by clay sediments. Results of butch studies testified that TCE degradation in ORR clayey soil corresponds to a pseudo-first-order kinetic model with reaction rate constants (k) of 0.05–0.24 day^{-1} at varied iron-to-soil ratios. Despite of elevated reactivity in water phase, the BNP were less effective in the site-derived clay sediment resulting calculated TCE removal efficiencies of 98.7% and 19.59%, respectively.

Transformations of ketones using stabilized nZVI and bimetallic Fe NPs are known. Among these catalytic processes, we note that porous Pt-Fe bimetallic nanocrystals were found to effectively facilitate the manufacturing of 2-propanol from acetone [70]. It was suggested that the high reactivity is strictly related to the interface consist of bimetallic Pt-Fe alloy and the Fe_2O_{3-x}. As an example of reduction of substituted aromatic ketones to alcohols, iron nanoparticles (size 9 nm, 14 nm, and 17 nm), stabilized by polyethylene glycol (PEG), carboxymethyl cellulose (CMC), and poly N-vinyl pyrrolidone (PVP), were used as catalysts in the hydrogenation reaction of various substituted aromatic ketones to alcohols with $NaBH_4$ [71]. Fe-PEG NPs were found to act as better catalyst than Fe-CMC NPs and Fe-PVP NPs. The trend in the catalytic activity among metals falls in the line of decreasing size effect of the nanoparticles i.e., the order of the nanoparticle sizes increase as Fe-PEG < Fe-CMC < Fe-PVP. Also, effects of substituents in the aromatic ring of ketones revealed that +I substituents are better catalyzed than –I substituents. In addition, bimetallic ruthenium-iron nanoparticles constitute a magnetically recoverable heterogeneous catalyst for transfer hydrogenation with a pronounced selectivity for ketones over aldehydes and nitro groups [72]. The nanoparticles are recyclable up to five times without significant decrease in activity or leaching.

Other processes. An Fe group ternary nanoalloy FeCoNi (NA) catalyst (its synthesis see Fig. 3) enabled selective electrocatalysis towards CO_2-free power generation from highly deliverable ethylene glycol (EG) [73]. This FeCoNi nanoalloy catalyst exhibited the highest selectivities toward the formation of C_2 products and to oxalic acid, *i.e.*, 99% and 60%, respectively, at 0.4 V vs. the reversible hydrogen electrode (RHE), without CO_2 generation. The key feature was the formation of an atomically mixed FeCoNi alloy to enhance the synergetic effect of the Fe group elements on anti-self-oxidation and selective oxidation of EG to oxalic acid. Reduction processes also required polymetallic particles. Thus, trimetallic core/shell Pd/FePt NPs were applied in oxygen reduction reaction (ORR) catalysis [74]. The uniform FePt shell was formed by controlled nucleation of $Fe(CO)_5$ in the presence of a Pt salt and Pd NPs at designated reaction temperatures.

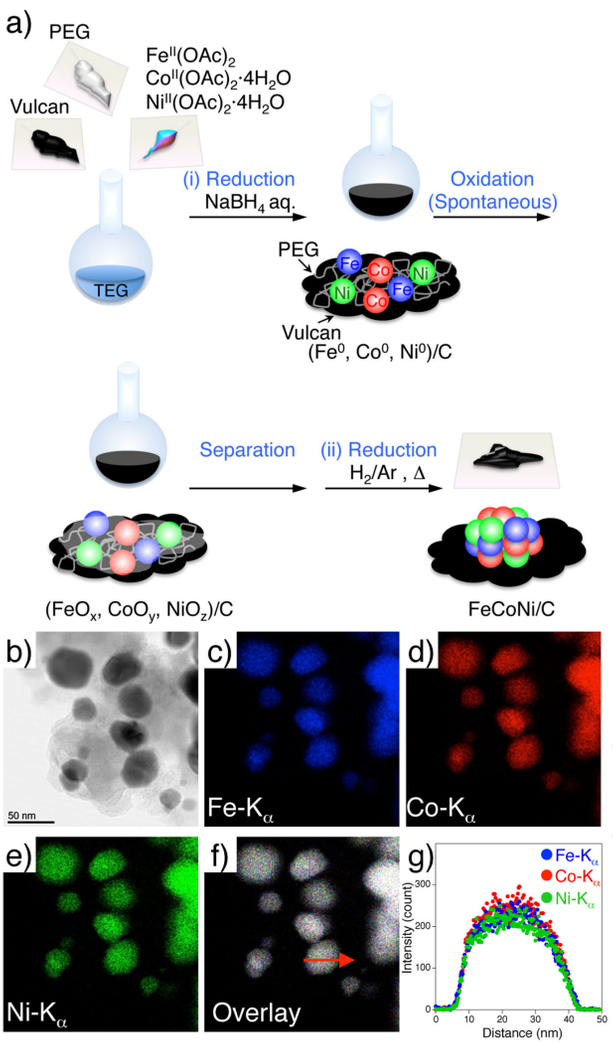

Figure 3. Synthetic scheme for the preparation of a FeCoNi nanoalloy catalyst supported on carbon (FeCoNi/C). Metallic Fe, Co and Ni form in the presence of polyethylene glycol (PEG) and a carbon support (vulcan) after the addition of an aqueous solution of $NaBH_4$. The metallic species are oxidised spontaneously, with production of an oxide mixture composed of Fe_3O_4, Co_3O_4, NiO, and so on is produced. FeCoNi/C was prepared by hydrogen reduction of the oxide mixture. Adapted from Matsumoto et al., 2014 with permission.

Iron-iron oxide core–shell nanoparticles were used as a catalyst for the *hydrogenation of olefins and alkynes* (reaction 3) under mild conditions in ethanol and in an aqueous medium [75]. The system is active in respect of a row of substrates and considerably selective for alkenes and alkynes over aromatic and carbonyl groups. The authors supposed that the presence of an oxide shell does not decrease its activity and provides a certain protection against oxidation by oxygen and water. In addition, highly active and well-defined AuPt nanoalloys, supported on the surface of ellipsoidal Fe@SiO_2 nanoparticles, were prepared by a method involving the loading of Pt NPs on the Fe_2O_3@SiO_2 nanocapsules *via* Sn^{2+} linkage and reduction, then *in situ* fabrication of Au nanoparticles by the galvanic replacement reaction between Au and Pt, and finally calcination and reduction to convert the nonmagnetic Fe_2O_3 to Fe core with high saturation magnetization [76]. The obtained Fe@SiO_2/AuPt samples exhibited a remarkably higher catalytic activity in comparison with the supported monometallic counterparts toward the *reduction of 4-nitrophenol to 4-aminophenol* by $NaBH_4$. The catalyst can be reused for several cycles with convenient magnetic separation.

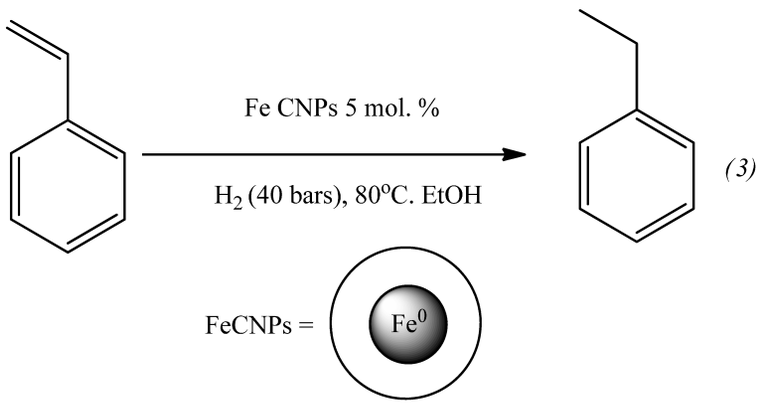

Hydrogenation of olefin catalyzed by Fe CSNPs.

3.3. Nano-Fe_2O_3 phases and their composites

Destruction of dangerous substances and pollutants. As well as Fe(0)-containing nanocomposites, oxidated iron forms are successfully used for degradation of several substances, both inorganic and organic. Thus, the decrease in temperature of *decomposition of ammonium perchlorate* in the presence of nano-ferric oxide was investigated [77] (see also section below on ferrites). It was shown that addition of nanometer-sized ferric oxide leads to a significant decrease in higher decomposition temperature of ammonium perchlorate. The catalytic activity of a colloidal catalyst (based on iron(III) oxides and obtained by hydrolysis followed by peptization of $FeCl_3 \cdot 6H_2O$ salt in water in the presence of 1% ethanol) in *decomposition of* H_2O_2 was studied [78]. The obtained catalyst is mainly composed of α-Fe_2O_3 crystals with an admixture of other crystalline structures of iron oxides, as well as carbon-containing compounds. Its activity with respect to H_2O_2 decomposition varies nonlinearly and nonmonotonically and its particle size grows starting from 1–3 nm with an increase in the initial

concentration of $FeCl_3 \cdot 6H_2O$ used to synthesize the catalyst. In addition, thermal decomposition of silver acetate at 200 °C in the presence of iron oxide microspheres in diphenyl ether led to the formation of iron oxide@Ag core–shell nanoparticles, exhibiting superparamagnetic behavior with a blocking temperature of about 42 K [79]. Their good catalytic activity and magnetic recovery was demonstrated by using two reactions, namely, *reduction of 4-nitrophenol* and *reduction of methylene blue* in aqueous solution. An especial case is the use of iron oxide / TiO_2 nanoparticles [80]. Thus, photocatalytic oxidation with TiO_2 nanoparticles (6–20 nm) was investigated as a promising water-treatment process [81, 82]. TiO_2 nanoparticles, after UV irradiation, are able to adsorb and degrade a huge variety of organic contaminants present in the environment. For example, in case of *organic arsenic species* (monomethylarsonic [MMA] and dimethylarsinic [DMA] acids), the strong affinity between the TiO_2 nanoparticles surface results a covalent bonding between MMA or DMA and the nanoparticle surface via formation of bidentate (AsMMA-Ti 3.32 Å) and monodentate (AsDMA-Ti 3.37 Å) inner-sphere complexes, respectively. Dopation of TiO_2 nanoparticles with Fe^{3+} ions at 0.1–0.5% may significantly increase the photocatalytic activity. The doped ions act as charge separators of the photoinduced electron–hole pair and enhanced interfacial charge transfers. Finally, an interesting application is known for *adsorption of elemental sulfur*. Thus, photoinduced sulfur desorption from the surfaces of Au Nps loaded on a series on metal oxides, in particular Fe_2O_3, was studied [83]. Elemental sulfur S_8 was selectively adsorbed on the Au Nps surfaces of Au/metal oxides in an atomic state. This phenomenon is applicable to the low temperature cleaning of sulfur-poisoned metal catalysts.

Organic synthesis. Free iron oxide(III) NPs and its nanocomposites have found numerous application in organic synthesis. Thus, hematite α-Fe_2O_3 NPs (diameters in the 7–18 nm range, synthesized by thermolysing a PVA-$Fe(OH)_3$ gel matrix at moderate temperatures) can effectively catalyze the *epoxidation of styrene* with *tert*-butyl hydroperoxide (TBHP) as the terminal oxidant [84]. Iron oxide nanoparticles supported on zirconia were tested in the gas-phase *conversion of cyclohexanol to cyclohexanone* in a fixed-bed flow type, Pyrex glass reactor, at 433–463 K [85]. Major detected products were cyclohexanone, cyclohexene and benzene, depending on the used catalyst. Experimental results showed that there was no leaching of metal, and that the catalyst was thus truly heterogeneous. In addition, core-shell Fe_2O_3/Pt nanoparticles with amorphous iron oxide cores exhibited superior catalytic activity with lower peak potential and enhanced CO_2 selectivity toward *methanol electrooxidation* in acidic medium [86]. This catalytic performance may be attributed to the uniform distribution of Pt particles on the amorphous Fe_2O_3 surface as well as interactions between the Pt particles and amorphous Fe_2O_3 cores. The catalytic activity of core-shell Fe_2O_3/Pt nanoparticles first increases and then decreases with decreasing Pt content. These nanomaterials also were found to have much higher structural stability and tolerance to the intermediates of methanol oxidation.

A magnetically separable core–shell iron oxide@nickel (IO@Ni) nanocatalyst, synthesized by reduction of Ni^{2+} ions in the presence of iron oxide (Fe^{2+}, Fe^{3+}) by a one-pot synthetic route using $NaBH_4$ as a reducing agent and starch as a capping agent, was found to have excellent activity for the *hydrogenation reactions* of aromatic nitro compounds under mild conditions using water

as a green solvent (reaction *4*). Excellent chemoselectivity and recyclability up to 30 cycles for the nitro group reduction was demonstrated. Nano propylsulphonated γ-Fe_2O_3 (NPS-γ-Fe_2O_3, reaction *5*) was applied as a magnetically recyclable heterogeneous catalyst for the efficient one-pot synthesis of bis(pyrazolyl)methanes in water (reaction *6*) [87]. The catalyst was easily isolated from the reaction mixture by a magnetic bar and reused at least five times without significant degradation in activity. Nanoporous α-Fe_2O_3 nanoparticles (about 100 nm in size and containing pores <10 nm) were synthesized *via* a hydrothermal method and applied in the catalytic *benzylation of benzene and benzyl chloride* (BC) in the fabrication of diphenylmethane (DPM) [88]. The BC conversion reached 100% in a reaction time of 3 min with 97.76% selectivity to DPM. The nanoporous α-Fe_2O_3 nanoparticles also have potential applications in other Friedel-Crafts alkylations, especially in large molecular reactions. Another example is related with chemical recycling of PET. Thus, easily recoverable superparamagnetic γ-Fe_2O_3 nanoparticles (10.5 nm in size and 147 $m^2 \cdot g^{-1}$ surface area, produced by calcining Fe_3O_4 nanoparticles prepared by the co-precipitation method) were used as a reusable catalyst for *PET glycolysis* [89]. At 300°C and a 0.05 catalyst/PET weight ratio, the maximum bis(2-hydroxyethlyl) terephthalate (BHET) monomer yielded reached more than 90% in 60 min. The catalyst was reused 10 times, giving almost the same BHET yield each time. In addition, heterogeneous photo-Fenton reaction which utilizes nanosized iron oxides as catalyst for maximizing the activity due to the enhanced physical or chemical properties brought about by the unique structures was described [90].

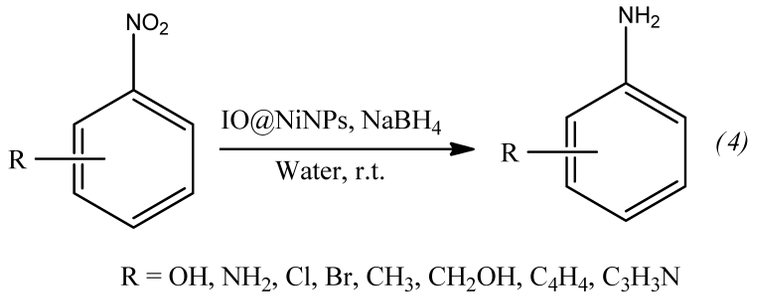

General scheme for the reduction of various nitroaromatics.

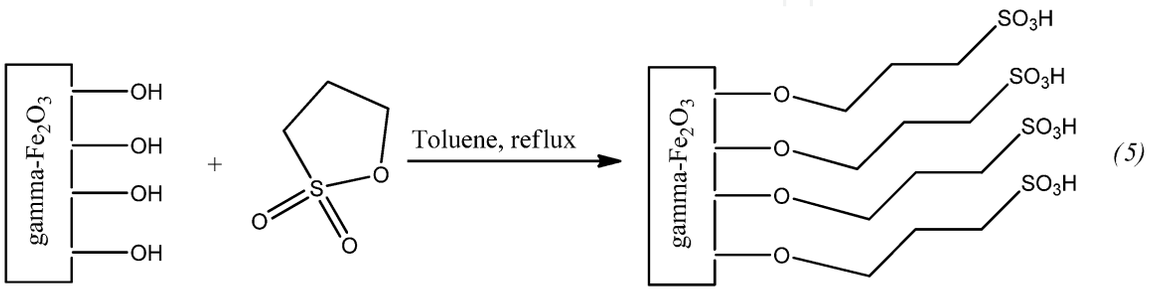

Synthesis of NPS-γ-Fe_2O_3.

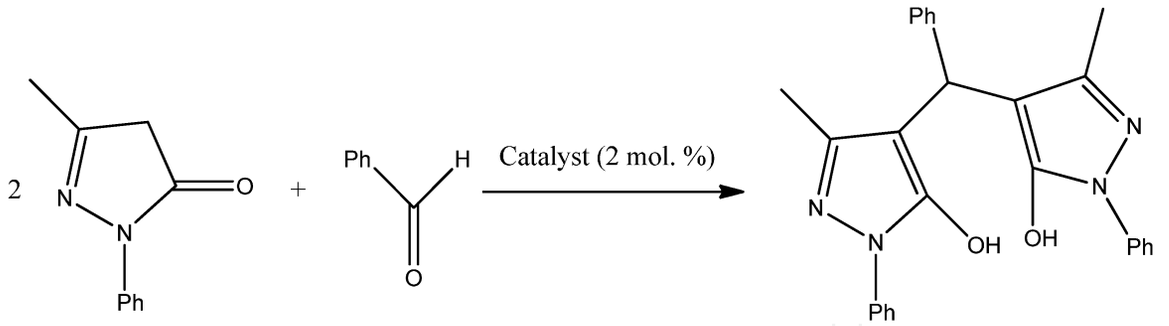

(6)

The reaction of benzaldehyde with 1-phenyl-3-methyl-5-pyrazolone.

Antibacterial activities. The doping effects of silver(I) and iron(III) on photocatalytic results using TiO_2 thin films were studied [91]. Ag and Fe doping and co-doping contents on nano-titania photocatalytic bactericidal films were obtained by sol-gel technique, thus uniting three classic active antibacterial species (Ag, Fe and TiO_2). The photocatalytic activity of TiO_2 films was confirmed by the sterilizing rate of the *E-coli* in each case. Applying fluorescent light irradiation, the optimal doping amounts of silver(I)/titania and iron(III)/titania were found to be 0.05% and 0.1%, respectively. In addition, a photocatalytic technique using visible light and carbon nanotubes and nano-sized Fe_2O_3 powder was used to *inhibit pathogenic bacterial growth* in water [92]. It was suggested that after careful design, this system can be used to disinfect drinking water, making it free of pathogenic bacteria.

3.4. Nano-Fe_3O_4 phases and their composites

Iron(II,III) oxide based nanostructures are slightly less explored in the organic synthesis. Thus, haemin-functionalized magnetic iron(II,III) oxide nanoparticles (Fe_3O_4/haemin) exhibited pronounced electrocatalytic activity towards *trichloroacetic acid* (TCA) like haemin itself (a linear detection range of 5–80 M and a detection limit of 0.3 M at 60 °C) [93]. This activity towards TCA was affected by detection temperature, which was controlled via electrically heated carbon paste electrodes. The maximal catalytic current was 5.8 times higher at 60 °C than at room temperature (25 °C). A process capable of synthesizing minor fractions of *aromatic hydrocarbons* (benzene, toluene, xylenes, and mesitylene) from CO_2 and H_2 at modest temperatures (T = 380 to 540°C) employing Fe/Fe_3O_4 nanoparticles as catalyst was designed [94]. The authors consider this technology as principally compatible with solar heat and hydrogen technology and having the potential to mitigate the impacts of global warming by making use of the existing distribution technology for gasoline. Also, *trisubstituted imidazoles* can be synthesized condensation reaction from 1,2-diketones, aromatic aldehydes, and ammonium acetate (reaction *7*) in high yield in the presence of sulphamic acid functionalized magnetic Fe_3O_4 nanoparticles (reaction *8*) as a solid acid catalyst under solvent-free classical heating conditions or using microwave irradiation [95].

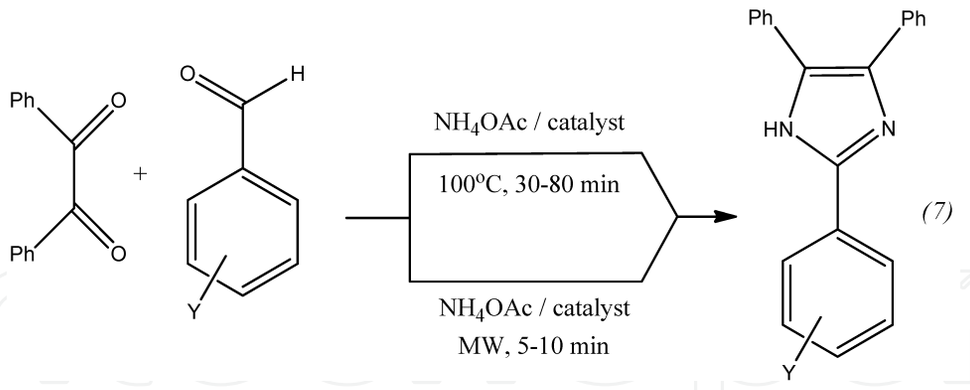

One-pot synthesis of 2,4,5-trisubstituted imidazoles catalyzed by sulphamic acid functionalized magnetic Fe_3O_4 nanoparticles under conventional heating conditions or using microwave irradiation.

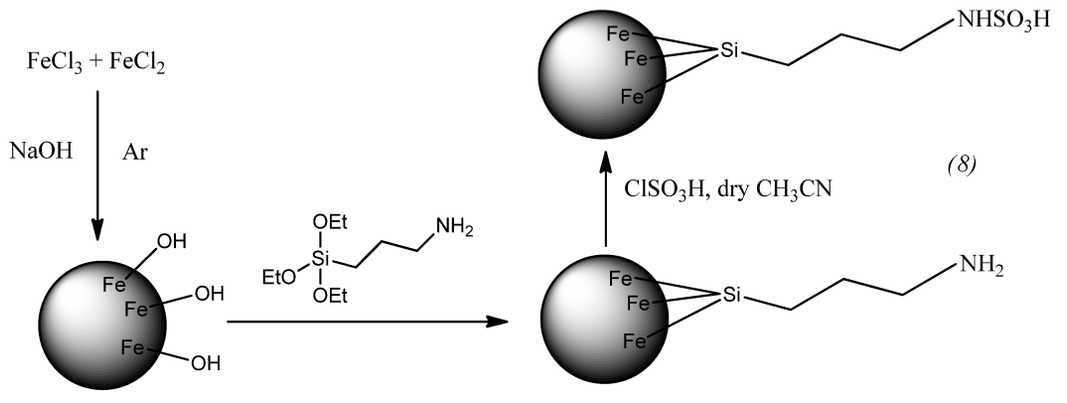

Preparation steps for fabricating sulphamic acid functionalized magnetic Fe_3O_4 nanoparticles.

Among other reactions, we note an efficient one-pot, three-component condensation reaction between 4-hydroxycoumarin, aryl glyoxals, and malononitrile catalyzed by Fe_3O_4 nanoparticles, which was carried out for the synthesis of several *dihydropyrano[c]chromenes* [96]. Also, an inexpensive and non-hazardous sulfuric acid functionalized magnetic Fe_3O_4 nanoparticles (efficiently catalyze one-pot multicomponent condensation of β-naphthol with aromatic and aliphatic aldehydes and amide derivatives (reaction *9*) at 100 °C under solvent-free conditions to afford the corresponding *amidoalkyl naphthols* in excellent yields and in very short reaction times [97]. Silver(0) nanoparticles supported on silica-coated Fe_3O_4 (synthesis see reactions *10*) serve as an efficient and recyclable heterogeneous catalyst for oxidant-free *dehydrogenation of alcohols* to the corresponding carbonyl compounds [98]. The catalyst can be easily recovered and reused for 8 reaction cycles without considerable loss of activity. At last, a nanocomposite of functionalized Ni(II) complex containing surface of pyridine, methoxysilanyl and amino groups with iron(II,III) oxide, Fe_3O_4@[-Ni(bpy)$_2$(py-tmos)] was found to be highly efficient green catalyst for the synthesis of a diverse range of 3,4-dihydropyrimidin-2(1H)-ones under solvent free conditions, and in addition it could be easily recovered by a simple magnetic separation and recycled at least 5 times without deterioration in catalytic activity [99].

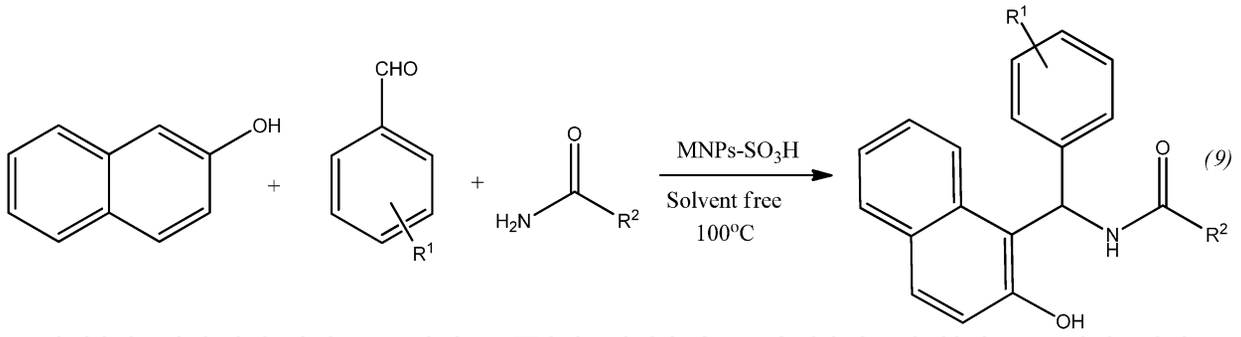

Synthesis of amidoalkyl naphthols

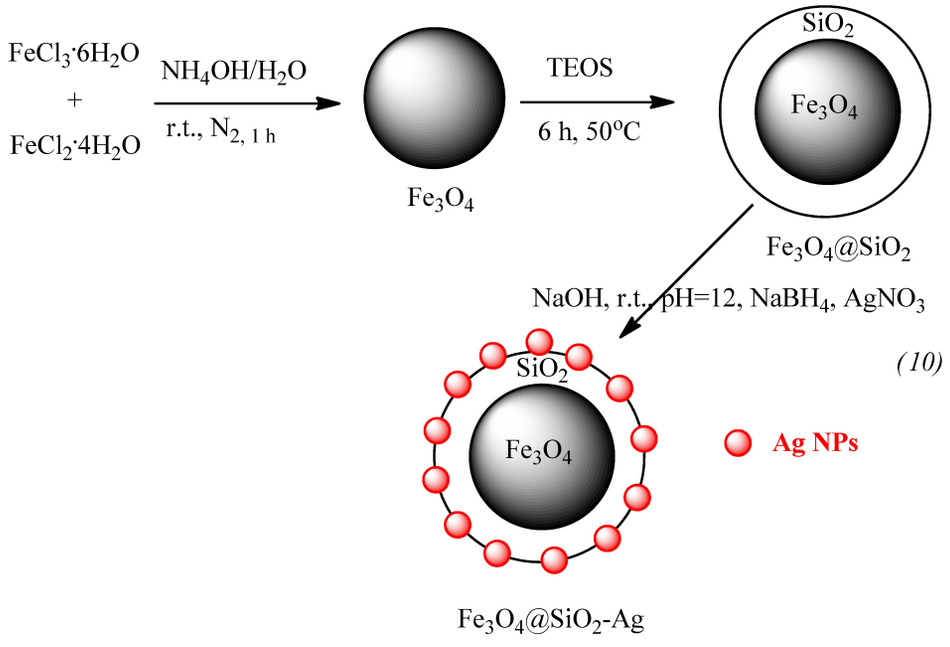

Preparation of magnetically recoverable heterogeneous nanocatalyst Fe_3O_4@SiO_2-Ag.

3.5. Ferrites

Cobalt ferrites having different sizes, from ultrasmall (2 nm) to 50 nm, can be fabricated by distinct techniques [100], mainly co-precipitation method (CPM), sometimes without using any capping agents/surfactants. Thus, the CPM was used to synthesize ultrasmall $CoFe_2O_4$ superparamagnetic nanoparticles (SPMNPs, 2–8 nm of an average size and high surface area of 140.9 m^2/g) without any surfactant [101]. Their catalytic activity was verified in the preparation of *arylidene barbituric acid derivatives* (reaction *11*) applying $CoFe_2O_4$ SPMNPs in aqueous ethanol as a reusable catalyst, which can be magnetically separated from the reaction system. Main advantages of this approach were found to be high yields, short reaction time and high turnover frequency, a clean reaction methodology, and chemoselectivity, among several others. More large-size $CoFe_2O_4$ magnetic nanoparticles (25 nm) were used as a catalyst for the

oxidation of various alkenes in the presence of *tert*-butylhydroperoxide (*t*-BuOOH) with almost quantitative yields (reaction *12*) [102]. It seemed that this heterogeneously catalysis system proceeds by coordination of *t*-BuOOH to the metal (Fe^{3+} cations) on the surface of the catalyst. The separation of the catalyst from the reaction media was easily achieved with the aid of an external magnet, and the catalyst can be reused several times with no loss of activity. In addition, combination of synthesis techniques can also be used for cobalt ferrite preparation. Thus, synthesis of spinel $CoFe_2O_4$ MNPs (average sizes 40–50 nm) was achieved by a combined sonochemical and co-precipitation technique in aqueous medium, also without any surfactant or organic capping agent [103]. These uncapped NPs were utilized directly for *aldol reaction* in ethanol (reaction 13). After the reaction was over, the nanoparticules were compartmented by using an external magnet.

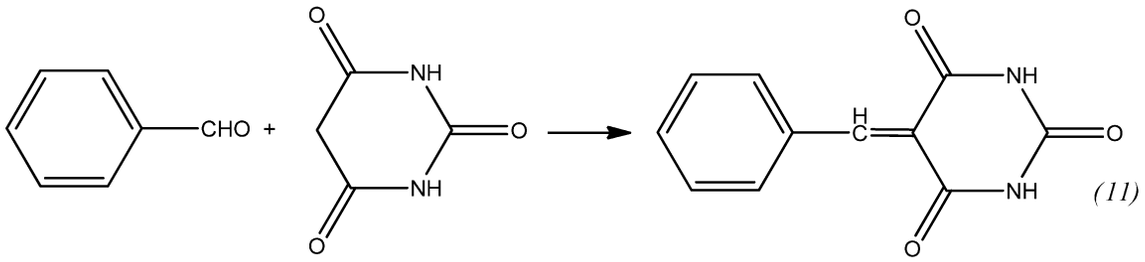

Optimization of reaction conditions using $CoFe_2O_4$ nanocatalyst. Yields 40–95%, best results in EtOH.

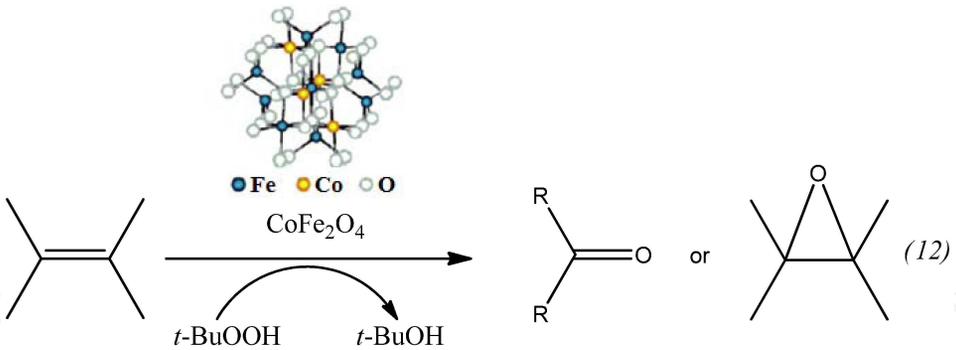

Oxidation of alkenes using $CoFe_2O_4$ catalyst.

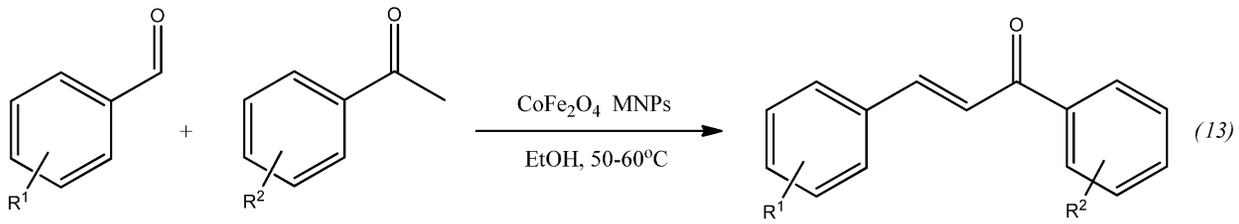

Figure 4. Aldol condensation reaction in presence of cobalt ferrite MNPs.

Nickel ferrites. Pure or doped nickel ferrites out of the nano-range size are common and frequently used in several catalytic processes. For instance, high reactivity of $NiFe_2O_4$ (111) surfaces (higher that in Fe_3O_4) is well-known; $NiFe_2O_4$ is an effective metal-doped ferrite catalyst in a typical industrial process such as the water-gas shift (WGS) reaction [104]. Similarly, $NiFe_2O_4$ was examined as catalyst in photocatalytic water oxidation using $[Ru(bpy)_3]^{2+}$ as a photosensitizer and $S_2O_8^{2-}$ as a sacrificial oxidant [105]. The catalytic activity of $NiFe_2O_4$ is comparable to that of a catalyst containing Ir, Ru, or Co in terms of O_2 yield and O_2 evolution rate under ambient reaction conditions. As an example of non-nano-sized doped ferrites, their catalysts (granules of ~1 mm diameter) of nickel, cobalt and copper, prepared by co-precipitation hydrothermal route and impregnated with palladium, cerium and lanthanum as promoters [106], were tested for carbon monoxide oxidation activities. The catalysis of $NiFe_2O_4$ nanoparticles on the *hydrogen storage performances* of magnesium hydride synthesized by high-energy ball milling was studied [107], showing that the initial dehydrogenation temperature of 7 mol.% $NiFe_2O_4$-doped MgH_2 is 191°C, which is 250°C lower than that of pristine MgH_2. The enhancement in the H_2 storage performances of MgH_2 by adding $NiFe_2O_4$ nanoparticles is primarily ascribed to intermetallic Fe_7Ni_3 and (Fe, Ni) phases during the desorption procedure, which act as the real catalyst in the 7 mol.% $NiFe_2O_4$-doped sample. As an example of another application, a magnetic acidic catalyst comprising Preyssler ($H_{14}[NaP_5W_{30}O_{110}]$) heteropoly acid supported on silica coated nickel ferrite nanoparticles ($NiFe_2O_4@SiO_2$) was investigated for the synthesis of *bis(dihydropyrimidinone)benzene and 3,4-dihydropyrimidin-2(1H)-ones derivatives* by the Biginelli reaction [108]. With the catalyst, the reactions occurred in less than 1 h with good to excellent yields.

Copper ferrites. Non-nanosized range copper ferrites have certain catalytic applications, such as, for example, for CO conversion to CO_2 [109]. In a difference of pure nickel ferrites, copper ferrite NPs are applied in organic catalysis in more uniform particle size (mainly about 20 nm). Thus, nano material on the basis of copper ferrite (20 nm) was applied as reusable heterogeneous initiator in the preparation of 1,4-dihydropyridines. The interaction of substituted *aromatic aldehydes, ethyl acetoacetate and ammonium acetate* (reaction *14*) was observed in presence of $CuFe_2O_4$ nano powders in ethanol at ambient conditions. The nano catalyst can be magnetically recovered and reused [110]. The same 20-nm size copper ferrite nano material also was reported as reusable heterogeneous initiator in the synthesis of β,γ-unsaturated ketones and allylation to acid chlorides in THF at r.t. without any additive/co-catalyst (reactions 15–16) [111]. The notable advantages are less expensive, heterogeneous reusable catalyst; mild reaction conditions, high yields of products, shorter reaction times, no isomerization during the reaction, and easy workup. In addition, 20-nm $CuFe_2O_4$ was applied as reusable heterogeneous initiator in the synthesis of *α-aminonitriles* by one-pot reaction of different aldehydes with amines and trimethylsilyl cyanides at r.t. in water as a solvent (reactions *17–18*) [112]. α-Aminonitriles are important in preparing a wide variety of amino acids, amides, diamines, and nitrogen containing heterocycles. In addition, a strategy for the synthesis of *benzoxazoles* from substituted N-(2-halophenyl)benzamides (reaction *19*) was developed [113], where inexpensive, readily available, air-stable, recyclable copper(II) ferrite serves as a nanocatalyst. Also, larger-size cubic copper ferrite $CuFe_2O_4$ nanopowders (24–51 nm in size) were synthesized *via* a hydrothermal route using industrial wastes (ferrous sulfate containing free sulfuric

acid ≈10%, 0.01% Zn^{2+} and 2% silica; copper waste 12.5% Cu, 8.7% Cl^- with minor Ni 0.001%) [114]. Study of photocatalytic degradation of the *methylene blue* (MB, $C_{16}H_{18}ClN_3S$) dye using copper ferrite powders showed a good catalytic efficiency (95.9%) at hydrothermal temperature 200 °C for hydrothermal time 24 h at pH = 12 due to high surface area (118.4 m^2/g).

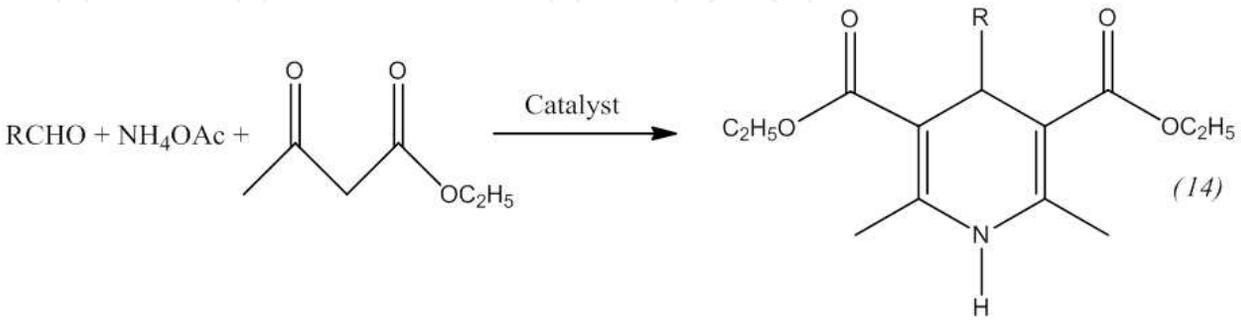

Catalyst: Copper ferrite (1 mol.%), R = a) Ph, b) 4-Me-*o*-C_6H_4, c) 4-ClC_6H_4, d) 4-NO_2-C_6H_4, e) 4-MeC_6H_4, (f) 3-NO_2-C_6H_4, (g) *n*-C_9H_9, (h) 2-NO_2-C_6H_4, (i) 2-furyl, (j) 2-Me-*o*-C_6H_4.

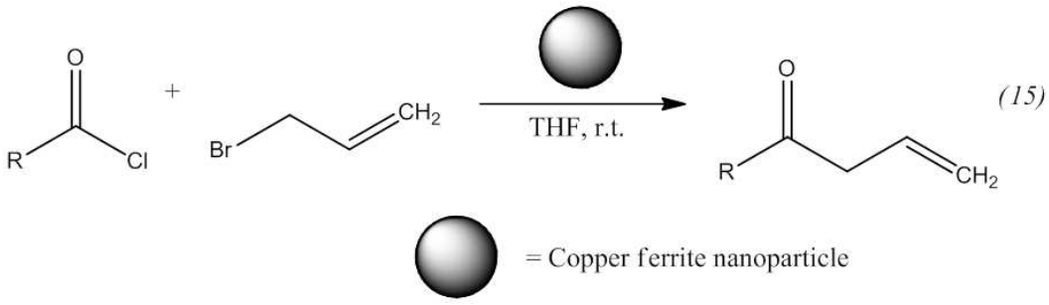

Synthesis of β,γ-unsaturated ketone using allyl bromide. R = (a) C_6H_5, (b) 2-ClC_6H_4, (c) 2-Br, 5-F, C_6H_3, (d) 2-Br, 5-F, C_6H_3, (e) furanyl, (f) 5-phenyl, 3-Methyl, 4-Isoxazolyl, (g) 5-(2,5-dichloro)phenyl, 3-methyl, 4-isoxazolyl, (h) $(CH_3)_3C$-, (i) $C_{11}H_{23}$-, (j) $C_{15}H_{31}$-.

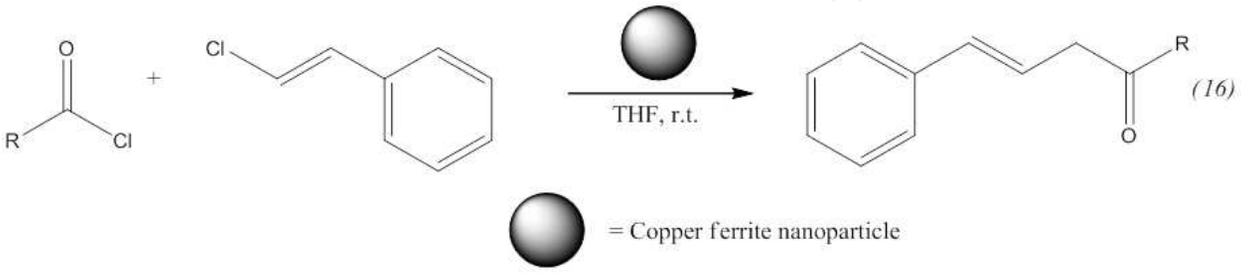

Synthesis of β,γ-unsaturated ketone using cinnamyl chlorides. Synthesis of β,γ-unsaturated ketone using cinnamyl chlorides. R = (a) C_6H_5, (b) 2-ClC_6H_4, (c) furanyl, (d)-$CH(CH_3)_2$.

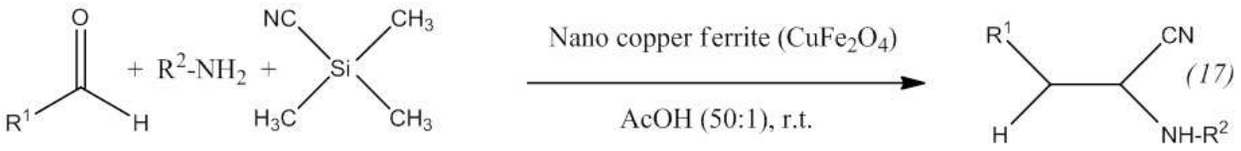

The synthesis of α-aminonitriles in the presence of nano $CuFe_2O_4$ in water as green solvent at r.t.

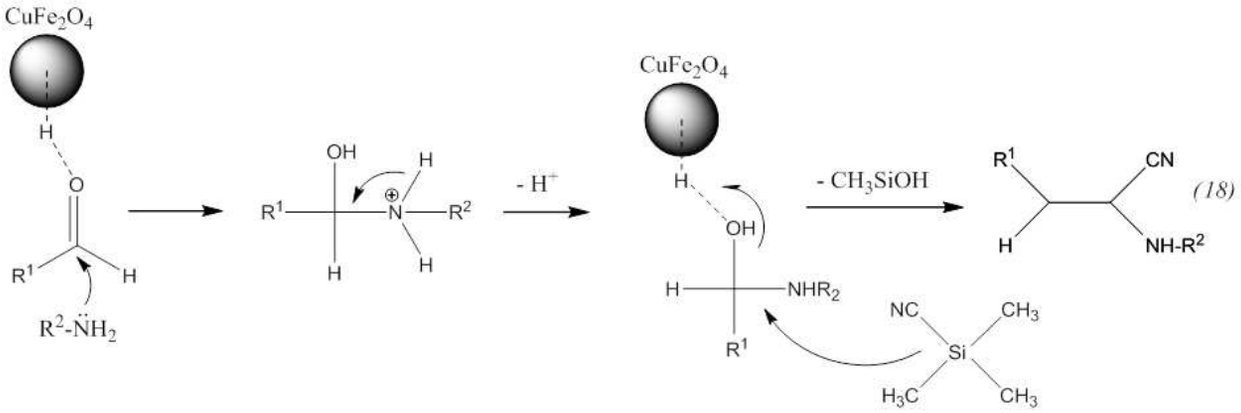

Suggested mechanism for the synthesis of α-aminonitriles derivatives in presence of acidic nano copper ferrite.

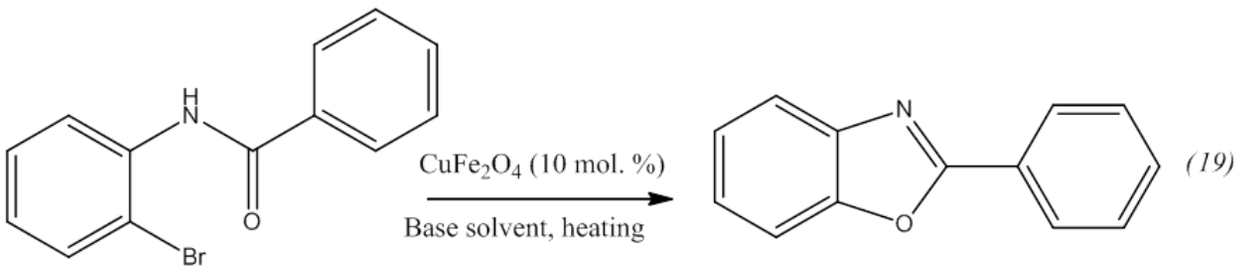

Catalyzed cyclization of N-(2-bromophenyl)benzamide to 2-phenyl-1,3-benzoxazole.

Zinc ferrite. Non-nano-sized zinc ferrites ($ZnFe_2O_4$) have been used in oxidative organic reactions. Thus, the catalytic behavior for *oxidative conversion of methane and oxidative coupling of methane* was investigated over pure and neodymium substituted zinc ferrites prepared by combustion method [115]. The catalytic activity proved to be strongly related to the oxide structure as well as to the specific defects created by substitution. The pure zinc ferrite ($ZnFe_2O_4$) and $ZnNd_2O_4$ exhibited high activity for coupling reaction whereas the neodymium substituted ferrites ($ZnFe_{1.75}Nd_{0.25}O_4$, $ZnFe_{1.5}Nd_{0.5}O_4$ and $ZnFeNdO_4$) was low active in this reaction. The order of the catalytic activities expressed as yields to C_2^+ were $ZnNd_2O_4$ > $ZnFe_2O_4$ > $ZnFe_{1.75}Nd_{0.25}O_4$ > $ZnFeNdO_4$ > $ZnFe_{1.5}Nd_{0.5}O_4$.

Analyzing pure zinc ferrite nanocatalysts, we note that mainly ultrasmall particles are currently applied in catalytic purposes. Thus, a nanosized highly ordered mesoporous zinc ferrite (ZF, 7–10 nm in size) was synthesized *via* co-precipitation method, further sulfated

with ammonium sulfate solution to obtain sulfated ZF (SZF) and was used for the synthesis of nopol by Prins condensation of *β*-pinene and paraformaldehyde (reaction *20*) [116]. 70% *conversion of β-pinene* with 88% selectivity to nopol was observed; the spent catalyst was regenerated and reused successfully up to four cycles with slight loss in catalytic activity. The influence of various reaction parameters such as solvent, reaction temperature, effect of substrate stoichiometry and catalyst loading was investigated. In particular, very low conversion (9%) of *β*-pinene was observed in protic solvents such as methanol (solvent effect); in case of apolar–aprotic solvents such as hexane, ethyl acetate and toluene, increase in the *β*-pinene conversion as well as nopol selectivity was observed. In case of reaction temperature, as the temperature increased to 110 °C, *β*-pinene conversion increased to 72% with slight drop in selectivity for nopol (57%). 95 °C was identified as optimal reaction temperature for further studies. At molar ratio of *β*-pinene to paraformaldehyde 1:3 molar ratio, maximum conversion was observed. The *β*-pinene conversion increased with an increase the catalyst loading (0.12 to 0.16 g) without affecting the nopol selectivity.

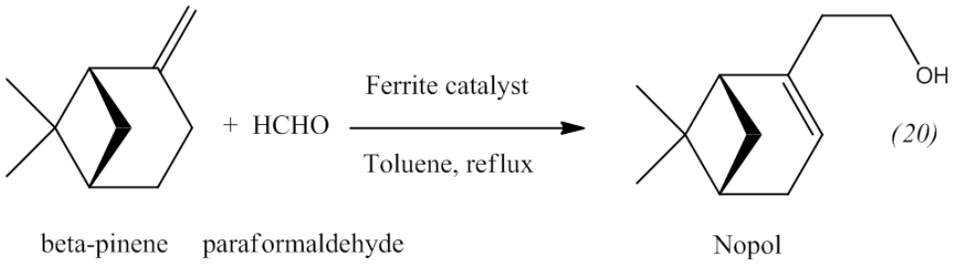

Prins condensation reaction of *β*-pinene and paraformaldehyde.

Other simple ferrites. The catalytic behavior of supported Au NPs for the process of *oxidation of benzyl alcohol* was elucidated in presence of gold nanoparticles [117]. Mg^{2+} ions, being present in the ferrite structure, led to an improvement of the catalytic activity of supported Au NPs to *ca*. 35% conversion, when an additional base was absent. Modifying the support with addition of MgO, the catalytic activity of supported Au nanoparticles was further improved to *ca.* 50% conversion; however, the catalyst was found to be deactivated in successive recycling tests. As well as nano-Fe_2O_3 mentioned above in the corresponding section, nano-$MnFe_2O_4$ particles (20–30 nm in size), synthesized by co-precipitation phase inversion method and low-temperature combustion method, using $MnCl_2$, $FeCl_3$, $Mn(NO_3)_2$, $Fe(NO_3)_3$, NaOH and $C_6H_8O_7$, were applied for thermal *decomposition of ammonium perchlorate* [118]. The catalytic mechanism was explained by the favorable electron transfer space provided by outer *d* orbit of transition metal ions and the high specific surface absorption effect of $MnFe_2O_4$ particles. Manganese ferrite nanoparticles were also applied in the synthesis of *spirooxindoles* (compounds **I-III**) *via* a one-pot and three-component reaction of isatins, malononitrile, and anilinolactones in the presence of a catalytic amount of $MnFe_2O_4$ NPs in PEG-400, as a nontoxic, green, and reusable solvent [119].

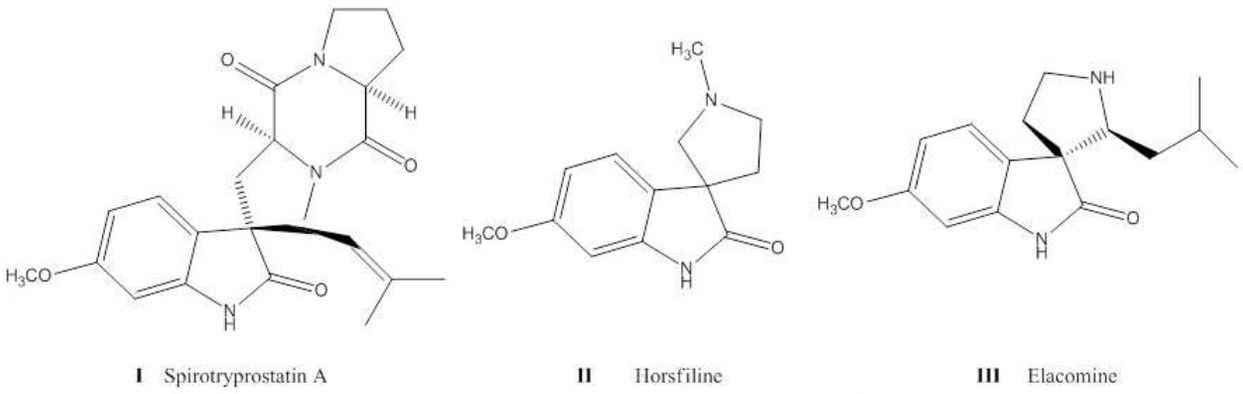

Selected spirooxindole natural products.

Mixed-metal or core-shell ferrites. Ferrites containing 2 metal ions, additionally to iron, are much more widespread in the nano-catalysis; their nanoparticle size can vary in a broad range, from ultrasmall particles (5–8 nm) up to 100 nm or more (in case of supported NPs). Both nano-sized and out-of-nano-sized mixed-metal ferrite NPs can be synthesized by a variety of methods, in particular classic sol-gel and co-precipitation methods or microwave heating ($MnZnFe_2O_4$ [120]).

***Cobalt**-based ferrite nanoparticles*. For cobalt-containing ferrite NPs, as well as for zinc ferrite above, one of important applications is the methanol decomposition to CO and hydrogen. Thus, $Cu_{1-x}Co_xFe_2O_4$ ($0<x<1$, 8–40 nm in size) was applied as a nanodimensional powder for this purpose [121]. The stabilization of the cubic structure with the substitution of copper ions by cobalt in mixed Cu-Co ferrites was observed. Cobalt containing ferrites exhibited higher and more stable catalytic activity and selectivity in *methanol decomposition* to CO and hydrogen in comparison with the $CuFe_2O_4$ one. Photocatalytic properties of the cobalt zinc ferrite $Co_{1-x}Zn_xFe_2O_4$ ($0<x<1$) nanoparticles (10.5–14.8 nm in size), prepared by a hydrothermal method, were studied on the example of *degradation of methyl blue* in aqueous solution [122]. It was elucidated that the oxidation-reduction potential of methyl blue aqueous solution in presence of the ferrite nano-particles at pH=7 under natural sunlight irradiation was negative and increased with increase in Zn content. The degradation rate of methyl blue also decreases as increase in Zn content in sunlight.

***Nickel**-based ferrite nanoparticles*. Similar to cobalt ferrites, several nickel-containing mixed or core-shell ferrites have been reported as nanocatalysts but in more narrow size range (18–50 nm). Thus, a magnetically separable catalyst consisting of ferric hydrogen sulfate (FHS) supported on silica-coated nickel ferrite nanoparticles (50 nm) was prepared [123]. This catalyst was shown to be an efficient heterogeneous catalyst for the *synthesis of 1,8-dioxodecahydroacridines* (reaction *21*) under solvent-free conditions. The catalyst can be recycled several times with no significant loss of catalytic activity.

Other mixed-metal ferrite nanoparticles. Ferrite nanoparticles, containing other metals and applied in the catalysis, are represented more chaotically in the available literature. Thus, the spinel ferrites $Cu_{1-x}Cd_x[Fe_{1-x}Al_xCr_{1-x}Mn_x]O_4$, where $0<x<1$, having unknown particle size, were

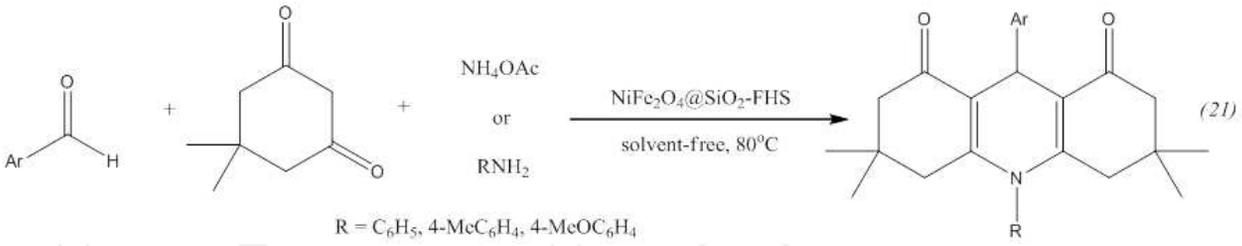

Synthesis of 1,8-dioxodecahydroacridines in the presence of $NiFe_2O_4$@SiO_2-FHS.

prepared by the coprecipitation technique [124]. Catalytic studies using *decomposition of* H_2O_2 as a model reaction between 303 and 343 K for 1–5 h using first order rate law suggested higher catalytic power for the composition $x = 0$ and then it decreases gradually. For the mixed spinel ferrite system $Mn_{1-x}Cu_xFe_2O_4$ ($x = 0, 0.25, 0.5, 0.75, 1.0$), the formation of phase pure spinels with FCC cubic structure with particle size ranging from 5.21 nm to 20 nm was observed at 333 K applying co-precipitation method with $MnCl_2$, $Fe(NO_3)_3 \cdot 9H_2O$ and $Cu(NO)_3 \cdot 3H_2O$ as precursors [125]. These ferrites were used as catalysts in the *alkylation of aniline*, showing a maximum conversion of 80.5% of aniline with selectivity of 98.6% towards N-methylaniline at 673 K, methanol/aniline molar ratio of 5:1 and weight hour space velocity of 0.2 h^{-1}. It was found that the yield is maximum for $CuFe_2O_4$. In addition, the catalytic performance of the ferrites was found to be proportional to surface area as well as acidity.

4. Conclusions

Iron-based nanoparticles, utilized in catalytic reactions described in this chapter, possess different sizes, from ultrasmall (2 nm) to 100 nm. They are obtained mainly by wet-chemical sol-gel or co-precipitation methods, sometimes combined with simple calcination at high temperatures, sonochemical technique, mechanical high-energy ball milling, or spark plasma sintering, among other methods. Microwave heating or hydrothermal route are also frequently used. Due to magnetic properties, these nano catalysts can be easily recovered from reaction systems and reused up to several runs almost without loss of catalytic activity.

Catalytic processes with application of iron-based nanocomposites are in a wide range. Notable attention is paid to methanol decomposition to CO and methane or to CO and hydrogen. Other catalyzed organic reactions consist of oxidation of various alkenes, aldol, alkylation and dehydrogenation reactions, synthesis of various organic compounds such as, for example, quinoxaline derivatives [126], β,γ-unsaturated ketones, arylidene barbituric acid derivatives, α-aminonitriles, nopol, 1,4-dihydropyridines, and 1,8-dioxodecahydro-acridines. Degradation/decomposition processes are also reported, for instance decomposition of H_2O_2 or photocatalytic degradation of methylene blue. Some of catalyzed reactions might have great practical applications, for instance transesterification of soybean oil to biodiesel. In addition, small iron-based particles could also be considered [127] as substituents of noble metals in a

variety of catalytic transformations. Several iron nanomaterials could have biological applications, such as peroxidase-like catalytic activity of Fe_3O_4 ultrasmall NPs [128].

We note that the total number of nano-iron composites applications for catalytic purposes is still not high, so it could be a perfect research niche for further applications of these nanomaterials in a variety of organic processes.

Author details

Boris I. Kharisov[1], Oxana V. Kharissova[1*], H.V. Rasika Dias[2], Ubaldo Ortiz Méndez[1], Idalia Gómez de la Fuente[1], Yolanda Peña[1] and Alejandro Vázquez Dimas[1]

*Address all correspondence to: okhariss@mail.ru

1 Universidad Autónoma de Nuevo León, Monterrey, México

2 The University of Texas at Arlington, Arlington, TX, USA

References

[1] Li, X.Q.; Elliott, D.W.; Zhang, W. Zero-Valent Iron Nanoparticles for Abatement of Environmental Pollutants: materials and engineering aspects. Crit. Rev. Solid State Mater. Sci. 2006, 31, 111–122.

[2] Hofmann-Amtenbrink, M.; von Rechenberg, B.; Hofmann, H. Superparamagnetic nanoparticles for biomedical applications. In: Nanostructured Materials for Biomedical Applications, 2009, Transworld Research Network, Kerala, India.

[3] Mahmoudi, M.; Sahraian, M. A.; Shokrgozar, M. A.; Laurent, S. Superparamagnetic Iron Oxide Nanoparticles: Promises for Diagnosis and Treatment of Multiple Sclerosis. ACS Chem. Neurosci. 2011, 2, 118–140.

[4] Huber, D. L. Iron nanoparticles, in: Dekker encyclopedia of nanoscience and nanotechnology, Schwarz, J. A.; Contescu, C. I.; Putyera, K., Eds., 2008, vol. 3, pp. 1681–1687, CRC Press, Taylor and Francis Group, Boca Raton, FL.

[5] C.S. Rajan.Nanotechnology in Groundwater Remediation. International Journal of Environmental Science and Development, 2011, 2(3), 182-187.

[6] Cheong, S.; Ferguson, P.; Hermans, I.F.; Jameson, G.N.L.; Prabakar, S.; Herman, D.A.J.; Tilley, R.D. Synthesis and Stability of Highly Crystalline and Stable Iron/Iron Oxide Core/Shell Nanoparticles for Biomedical Applications. ChemPlusChem, 2012, 77, 135–140.

[7] Harm, U.; Schuster, J.; Mangold, K.-M. Modification of iron nanoparticles for ground water remediation. DECHEMA, Karl-Winnacker Institut, 2010, http://kwi.dechema.de/kwi_media/Downloads/ec/F564_Nanoeisen_Harm.pdf.

[8] Bai J, Wang J-P. High-magnetic-moment core-shell-type FeCo-Au/Ag nanoparticles. Appl. Phys. Lett., 2005, 87(15), 152502/1-152502/3.

[9] Figuerola, A.; Di Corato, R.; Manna, L.; Pellegrino, T. From iron oxide nanoparticles towards advanced iron-based inorganic materials designed for biomedical applications. Pharmaceutical Research, 2010, 62(2), 126–143.

[10] Qing Wei Ding, Tian Wei Qian, Hong Fang Liu, Xue Wang. Preparation of Zero-Valent Iron Nanoparticles and Study of Dispersion. 2011, Applied Mechanics and Materials, 55–57, 1748–1752.

[11] Jae-min Lee; Ji-hun Kim; Jin-wook Lee; Jae-hwan Kim; Ho-seok Lee; Yoon-seok Chang. Synthesis of Fe-nano Particles Obtained by Borohydride Reduction with Solvent. Paper A-068, in: Bruce M. Sass (Conference Chair), Remediation of Chlorinated and Recalcitrant Compounds—2008. Proceedings of the Sixth International Conference on Remediation of Chlorinated and Recalcitrant Compounds (Monterey, CA; May 2008). ISBN 1-57477-163-9, published by Battelle, Columbus, OH, www.battelle.org/chlorcon.

[12] Khodabakhshi, A.; Amin, M.M.; Mozaffari. M. Synthesis of magnetite nanoparticles and evaluation of its efficiency for arsenic removal from simulated industrial wastewater. Iran. J. Environ. Health. Sci. Eng., 2011, 8 (3), 189–200.

[13] Park, H.; Ayala, P.; Deshusses, M.A.; Mulchandani, A.; Choi, H.; Myung, N.V. Electrodeposition of maghemite (γ-Fe_2O_3) nanoparticles. Chem. Eng. J., 2008, 139, 208–212.

[14] Grabis, J.; Heidemane, G.; RAŠMANE, D. Preparation of Fe_3O_4 and γ-Fe_2O_3 Nanoparticles by Liquid and Gas Phase Processes. Mat. Sci. (MEDŽIAGOTYRA). 2008, 14 (4), 292–295.

[15] Ballard, S.G. Apparatus and methods for the production of powders. US20056972115 (2005).

[16] Kim, W.-B., Park, J.-S., Suh, C.-Y., Kil, D.-S., Lee, J.-C. 2007, US20070209477.

[17] Lei, J.P.; Dong, X.L.; Zhu, X.G. et al. Formation and characterization of intermetallic Fe–Sn nanoparticles synthesized by an arc discharge method. Intermetallics, 2007, 15(12), 1589–1594.

[18] Gupta, M.; Wong, E.; Leong, W. Microwaves and metals. Wiley-Interscience, 2007, 256 pp.

[19] Komarneni, S.; Katsuki, H.; Li, D.; Bhalla, A.S. Microwave–polyol process for metal nanophases. J. Phys.: Condens. Matter., 2004, 16, S1305-S1312.

[20] Becker, M.F.; Brock, J.R.; Cai, H. et al. Metal nanoparticles generated by laser ablation. Nanostruct. Mater. 1998, 10(5), 853–863.

[21] Rodrigues, A.R.; Soares, J.M.; Machado, F.L.A.; de Azevedo, W.M.; de Carvalho, D.D. Synthesis of α-Fe particles using a modified metalmembrane incorporation technique. J. Magnetism Magnetic. Mat., 2007, 310(2), Part 3: 2497–2499.

[22] Klaine, S.J.; Alvarez, P.J.J.; Batley, G.E.; Fernandes, T.F.; Handy, R.D.; Lyon, D.J.; Mahendra, S.; Mclaughlin, M.J.; Lead, J.R. Nanomaterials in the environment: behavior, fate, bioavailability, and effects. Environmental Toxicology and Chemistry, 2008, 27(9), 1825–1851.

[23] Yuvakkumar, R.; Elango, V.; Rajendran, V.; Kannan, N. Preparation and characterization of zero-valent iron nanoparticles. Digest Journal of Nanomaterials and Biostructures, 2011, 6(4), 1771–1776.

[24] Bönnemann, H.; Brijoux, W.; Brinkmann, R.; Dinjus, E.; Joussen, T.; Korall, B. Erzeugung von kolloiden Übergangsmetallen in organischer Phase und ihre Anwendung in der Katalyse. Angew. Chem., 1991, 103, 1344–1346; Angew. Chem. Int. Ed. Engl., 1991, 30, 1312.

[25] Harutyunyan, A.; Grigorian, L.; Tokune, T. Method for synthesis of metal nanoparticles. 2005, US20056974493.

[26] Klinke, C.; Kern, K. Iron nanoparticle formation in a metal-organic matrix: from ripening to gluttony. Nanotechnology, 2007, 18, 215601.

[27] Lu, Y.; Zhu, Z.; Liu, Z. Carbon-encapsulated Fe nanoparticles from detonation-induced pyrolysis of ferrocene. Carbon, 2005, 43(2), 369–374.

[28] Anastas, P. T.; Horvath, I. T. Green Chemistry for a Sustainable Future. Wiley; 1st edition, 2012, 350 pp.

[29] Chao-Jun Li, Paul T. Anastas. Handbook of Green Chemistry — Green Processes. Wiley-VCH; 3 Volume Set edition, 2012, 1326 pp.

[30] Ahluwalia, V. K. Green Chemistry: Environmentally Benign Reactions, Second Edition. CRC Press; 2nd edition, 2012, 326 pp.

[31] Patel, J. T.; Patel, O. B.; Raval, B. P. Green Chemistry: New Avenues in Chemical Research: Focus in Healthcare. LAP LAMBERT Academic Publishing, 2012, 60 pp.

[32] Luque, R. Green Chemistry. Nova Science Publishers, 2011.

[33] Hoag, G. E.; Collins, J. B.; Varma, R. S.; Nadagouda, M. Green synthesis of metal nanoparticles using plant extracts. PCT Int. Appl. 2009, WO 2009140694 A2 20091119.

[34] Kipkurgat Erick Tanui. Green Synthesis and Characterization of Iron Nanoparticles. http://chemistry.uonbi.ac.ke.

[35] Yao, C.; Ma, H.; Tong, Y. Electrochemical preparation and magnetic study of amorphous nanostructured Nd-Fe-Co-Ni-Mn high entropy alloy film. Yingyong Huaxue, 2011, 28(10), 1189–1194.

[36] Glebov, A.V.; Glebov, V.A.; Popova, O.I. Development of nanofilm Fe-Pt magnets for superdense-recording heads. Tsvetnye Metally, 2009, (12), 67–70.

[37] Wang, J.; Cheng, R. Preparation and application of activated carbon supported iron nanomaterial, with application to pentachlorophenol degradation. 2010, CN 101708457.

[38] Bystrzejewski, M. Synthesis of carbon-encapsulated iron nanoparticles via solid state reduction of iron oxide nanoparticles. Journal of Solid State Chemistry, 2011, 184(6), 1492–1498.

[39] Wei, Z.; Wang, X.; Yang, H. Preparation of carbon-encapsulated Fe core-shell nanostructures by confined arc plasma. Materials Science Forum, 2011, 688(Nano-Scale and Amorphous Materials), 245–249.

[40] Rao, C.N.R.; Thomas, P.J.; Kulkarni, G.U. Nanocrystals: Synthesis, Properties and Applications (Springer Series in Materials Science). Springer, 2007, 182.

[41] Bingshe, X.; Junjie, G.; Xiaomin, W.; Xuguang, L.; Hideki, I. Synthesis of carbon nanocapsules containing Fe, Ni or Co by arc discharge in aqueous solution. Carbon, 2006, 14(13), 2631–2634.

[42] Nadagouda, M.N.; Lytle, D.A. Microwave-assisted combustion synthesis of nano iron oxide/iron coated activated carbon, anthracite, cellulose fiber, and silica, with arsenic adsorption studies. Journal of Nanotechnology, 2011, 972486, 8 pp.

[43] Yuliang An; Jieshan Qiu. Synthesis of carbon encapsulated iron nanoparticles by carbonization of starch with iron as catalyst. 2007, The American Carbon Society. http://acs.omnibooksonline.com/data/papers/2004_C085.pdf

[44] An Yuilang; Wu Xiaojuan; Sui Zhiming; yuan Xia, Liu yanqiu. A novel method for synthesis of homogeneous carbon encapsulated Fe nanoparticles based on natural biopolymer. J. Rare Earths, 2007, 25, 452.

[45] Salah El-Din, T.A.; Elzatahry, A.A.; Aldhayan, D.M.; Al-Enizi, A.M.; Al-Deyab, S.S. Synthesis and Characterization of Magnetite Zeolite Nano Composite. Int. J. Electrochem. Sci.,2011, 6, 6177–6183.

[46] Liu, H.; Lan, G.; Yan, Y.; Tang, H.; Liu, H.; Li, Y. Direct hydrothermal synthesis of novel ordered magnetic mesoporous nanocomposites with high content of iron. Gongye Cuihua, 2011, 19(8), 11–15.

[47] Shi, Y.-f.; Zhou, X.; Zhong, L.-b.; Xu, W.-l.; Wang, Y.; Zhang, Q.-q. Synthesis and formation mechanism of core-shell Fe_3O_4 coated gold nanomaterials. Dongnan Daxue Xuebao, Yixueban, 2011, 30(1), 6–10.

[48] Liu, X.; Xu, M.; Zhao, R.; Zhong, J. Iron phthalocyanine prepolymer/Fe_3O_4 nano hybrid magnetic material and its preparation method. Edited by: Casciano, D.A.; Sahu, S.C. Faming Zhuanli Shenqing, 2011, CN 102086304.

[49] Goodarz Naseri, M.; Saion, E.B.; Abbastabar Ahangar, H.; Halim Shaari, A.; Hashim, M. Simple Synthesis and Characterization of Cobalt Ferrite Nanoparticles by a Thermal Treatment Method. J. Nanomater. Volume 2010, Article ID 907686, 8 pp.

[50] Li, X.Q.; Elliot, D.W.; Zhang, W.X. Zero-valent iron nanoparticles for abatement ofenvironmental pollutants: materials and engineering aspects. Crit. Rev. Solid State, 2006, 31, 111–22.

[51] Pan, J.R.; Huang, C.; Hsieh, W.-P.; Wu, B.J. Reductive catalysis of novel TiO_2/Fe^0 composite under UV irradiation for nitrate removal from aqueous solution. Separation and Purification Technology, 2012, 84, 52–55.

[52] Kustov, L.M.; Al-Abed, S.R.; Virkutyte, J.; Kirichenko, O.A.; Shuvalova, E.V.; Kapustin, G.I.; Mishin, I.V.; Nissenbaum, V.D.; Tkachenko, O.P.; Finashina, E.D. Novel Fe-Pd/SiO_2 catalytic materials for degradation of chlorinated organic compounds in water. Pure Appl. Chem. 2014, 86(7), 1141–1158.

[53] Amir, A.; Lee, W.Enhanced reductive dechlorination of tetrachloroethene by nanosized zero valent iron with vitamin B12. Chem. Engin. J., 2011, 170, 492–497.

[54] Dror, I.; Jacov, O.M.; Cortis, A.; Berkowitz, B. Catalytic Transformation of Persistent Contaminants Using a New Composite Material Based on Nanosized Zero-Valent Iron. ACS Appl. Mater. Interfaces, 2012, 4, 3416–3423.

[55] Varanasi, P.; Fullana, A.; Sidhu, S. Remediation of PCB contaminated soils using iron nano-particles. Chemosphere, 2007, 66(6), 1031–1038.

[56] Dehghani, M., Shahsavani, E.; Farzadkia, M.; Reza Samaei, M. Optimizing photo-Fenton like process for the removal of diesel fuel from the aqueous phase. J. Environ. Health Sci. Eng., 2014, 12, 87.

[57] Messele, S.A.; Bengoa, C.; Stuber, F.; Fortuny, A.; Fabregat, A.; Font, J. Catalytic wet peroxide oxidation of phenol using nanoscale zero-valent iron supported on activated carbon. Desalination and Water Treatment, 2015, 55, 1–10. http://www.tandfonline.com/doi/full/10.1080/19443994.2014.1002011#preview

[58] Torres Galvis, H.M.; Bitter, J.H.; Khare, C.B.; Ruitenbeek, M.; Dugulan, A.I.; de Jong, K.P. Supported Iron Nanoparticles as Catalysts for Sustainable Production of Lower Olefins. Science, 2012, 335, 835.

[59] Zhang, C.; Zhou, L.; Yang, J.; Yu, X.; Jiang, Y.; Zhou, M.Nanoscale zero-valent iron/AC as heterogeneous Fenton catalysts in three-dimensional electrode system. Environ. Sci. Pollut. Res. 2014, 21, 8398–8405.

[60] Zhang, S.; Wang, D.; Zhang, X.; Fan, P. Zero-Valent Iron Immobilized on Multi-Walled Carbon Nanotubes for Heterogeneous Catalytic Ozonation of Methylene Blue as Model Compound. Clean – Soil, Air, Water, 2014, 42 (5), 609–616.

[61] Datta, K.K.R.; Petala, E.; Datta, K.J.; Perman, J.A.; Tucek, J.; Bartak, P., Otyepka, M.; Zoppellaro, G.; Zboril, R. NZVI modified magnetic filter paper with high redox and catalytic activities for advanced water treatment technologies. Chem. Commun., 2014, 50, 15673–15676.

[62] Varma, R.S. Nano-catalysts with magnetic core: sustainable options for greener synthesis. Sustainable Chemical Processes, 2014, 2, 11.

[63] Wei, S.; Wang, Q.; Zhu, J., Sun, L.; Line, H.; Guo, Z. Multifunctional composite core–shell nanoparticles. Nanoscale, 2011, 3, 4474–4502.

[64] Govan, J.; Gun'ko, Yu.K. Recent Advances in the Application of Magnetic Nanoparticles as a Support for Homogeneous Catalysts. Nanomaterials, 2014, 4, 222–241.

[65] Liu, W.-J.; Qian, T.T.; Jiang, H. Bimetallic Fe nanoparticles: Recent advances in synthesis and application in catalytic elimination of environmental pollutants. Chemical Engineering Journal, 2014, 236, 448–463.

[66] Hsieh, S.; Lin, P.-Y. FePt nanoparticles as heterogeneous Fenton-like catalysts for hydrogen peroxide decomposition and the decolorization of methylene blue. J. Nanopart. Res. 2012, 14, 956.

[67] Mao, Z.; Wu, Q.; Wang, M.; Yang, Y.; Long, J.; Chen, X. Tunable synthesis of SiO_2-encapsulated zero-valent iron nanoparticles for degradation of organic dyes. Nanoscale Research Letters, 2014, 9, 501.

[68] Li, Q.-x.; Sun, Z.-y.; Wang, T. Edited by: Casciano, D.A.; Sahu, S.C. A study on preparation, characterization and photocatalytic activity of iron-doped nano-TiO_2 thin films based on self-assembled monolayers. Kuangwu Xuebao, 2011, 31(1), 102–107.

[69] Katsenovich, Y.P.; Miralles-Wilhelm, F.R. Evaluation of nanoscale zerovalent iron particles for trichloroethene degradation in clayey soils. Science of the Total Environment, 2009, 407, 4986–4993.

[70] Ji, Y.; Wu, Y.; Zhao, G.; Wang, D.; Liu, L.; He, W.; Li, Y. Porous bimetallic Pt-Fe nanocatalysts for highly efficient hydrogenation of acetone. Nano Research, 2015, 8(8), 2706-2713. http://link.springer.com/article/10.1007%2Fs12274–015-0777-z

[71] Parimala, L.; Santhanalakshmi, J. Studies on the Iron Nanoparticles Catalyzed Reduction of Substituted Aromatic Ketones to Alcohols. Journal of Nanoparticles. Volume 2014, Article ID 156868, 10 pp.

[72] Hudson, R.; Chazelle, V.; Bateman, M.; Roy, R.; Li, C.; Moores, A. Sustainable synthesis of magnetic ruthenium-coated iron nanoparticles and application in the catalytic transfer hydrogenation of ketones. ACS Sustainable Chem. Eng., 2015, 3 (5), 814–820.

[73] Matsumoto, T.; Sadakiyo, M.; Lee Ooi, M.; Kitano, S.; Yamamoto, T.; Matsumura, S.; Kato, K.; Takeguchi, T.; Yamauchi, M. CO_2-Free Power Generation on an Iron Group Nanoalloy Catalyst via Selective Oxidation of Ethylene Glycol to Oxalic Acid in Alkaline Media. Sci. Reports, 2014, 4, 5620, 6 pp.

[74] Mazumder, V.; Chi, M.; More, K.L.; Sun, S. Core/Shell Pd/FePt Nanoparticles as an Active and Durable Catalyst for the Oxygen Reduction Reaction. J. Am. Chem. Soc. 2010, 132, 7848–7849.

[75] Hudson, R.; Riviere, A.; Cirtiu, C.M.; Luska, K.L.; Moores, A. Iron-iron oxide core–shell nanoparticles are active and magnetically recyclable olefin and alkyne hydrogenation catalysts in protic and aqueous media. Chem. Commun., 2012, 48, 3360–3362.

[76] Zhang, Z.; Zhou, Y.; Zhang, Y.; Zhou, S.; Xiang, S.; Sheng, X.; Jiang, P. A highly reactive and magnetic recyclable catalytic system based on AuPt nanoalloys supported on ellipsoidal Fe@SiO_2. J. Mater. Chem. A, 2015, 3, 4642–4651.

[77] Mahinroosta, M. Catalytic effect of commercial nano-CuO and nano-Fe_2O_3 on thermal decomposition of ammonium perchlorate. Journal of Nanostructure in Chemistry, 2013, 3, 47.

[78] Lesin, V.I.; Pisarenko, L.M.; Kasaikina, O.T. Colloidal Catalysts Based on Iron (III) Oxides. 1. Decomposition of Hydrogen Peroxide. Colloid Journal, 2012, 74 (1), 85–90.

[79] Sharma, G.; Jeevanandam, P. A Facile Synthesis of Multifunctional Iron Oxide@Ag Core–Shell Nanoparticles and Their Catalytic Applications. Eur. J. Inorg. Chem., 2013, 6126–6136.

[80] Zaleska, A. Doped-TiO_2: A Review. Recent Patents on Engineering, 2008, 2, 157–164.

[81] Aufan, M. Nanoparticules d'oxydes mrtalliques: relations entre la reactivite de surface et des reponses biologiques. http://www.tel.archives-ouvertes.fr/docs/00/30/85/03/PDF/auffan_PhD.pdfSimilares.

[82] Jing, C.; Xiaoguang Meng; Suqin Liu; Salem Baidas; Ravi Patraju; Christos Christodoulatos; George P. Korfiatis. Surface complexation of organic arsenic on nanocrystalline titanium oxide. Journal of Colloid and Interface Science, 2005, 290(1), 14–21.

[83] Tada, H.; Soejima, T.; Ito, S.; Kobayashi, H. Photoinduced desorption of sulfur from gold nanoparticles loaded on metal surfaces. J. Amer. Chem. Soc. 2004, 126(49), 15952–15953

[84] Bepari, R.A.; Bharali, P.; Das, B.K. Controlled synthesis of α-and γ-Fe_2O_3 nanoparticles via thermolysis of PVA gels and studies on α-Fe_2O_3 catalyzed styrene epoxidation. Journal of Saudi Chemical Society, 2014, In press.

[85] Sadiq, M.; Zamin, G.; Razia; Ilyas, M. Synthesis and Characterization of Iron Oxide Nanoparticles Supported on Ziconia and Its Application in the Gas-Phase Oxidation of Cyclohexanol to Cyclohexanone. Modern Research in Catalysis, 2014, 3, 12–17

[86] Liu, Y.-T.; Yuan, Q.-B.; Duan, D.-H.; Zhang, Z.-L.; Hao, X.-G.; Wei, G.-Q.; Liu, S.-B. Electrochemical activity and stability of core-shell Fe_2O_3/Pt nanoparticles for methanol oxidation. Journal of Power Sources, 2013, 243, 622–629.

[87] Sobhani, S.; Pakdin-Parizi, Z.; Nasseri, R. Nano n-propylsulphonated γ-Fe_2O_3: A novel magnetically recyclable heterogeneous catalyst for the efficient synthesis of bis(pyrazolyl)methanes in water. J. Chem. Sci. 2013, 125 (5), 975–979.

[88] Cuong, N.D.; Hoa, N.D.; Hoac T.T.; Khieu, D.Q.; Quang, D.T.; Quang, V.V.; Hieu, N.V. Nanoporous hematite nanoparticles: Synthesis and applications for benzylation of benzene and aromatic compounds. J. Alloys Comp. 2014, 582, 83–87.

[89] Bartolome, L.; Imran, M.; Lee, K.G.; Sangalang, A.; Keun Ahnd, J.; Hyun Kim, D. Superparamagnetic γ-Fe_2O_3 nanoparticles as an easily recoverable catalyst for the chemical recycling of PET. Green Chem., 2014, 16, 279–286.

[90] Wang, C.; Liu, H.; Sun, Z. Heterogeneous Photo-Fenton Reaction Catalyzed by Nanosized Iron Oxides for Water Treatment. International Journal of Photoenergy, 2012, Article ID 801694, 10 pp.

[91] Han, J.; Zhang, S.-j.; Lu, Z.-g.; Wang, Y.-j. Doping Fe^{3+} to nano-Ag TiO_2 for photocatalytic performance improvement. Yingyong Guangxue, 2010, 31(5), 718–723.

[92] Sharon, M.; Pal, B.; Kamat, D.V. Photocatalytic killing of pathogenic bacterial cells using nanosize Fe_2O_3 and carbon nanotubes. Journal of Biomedical Nanotechnology, 2005, 1(3), 365–368.

[93] Yin, Z.-Z.; Li, Y.; Jiang, L.-P.; Kumar Rana, R.; Jun-Jie Zhu. Synthesis and electrocatalytic activity of haemin-functionalised iron(II,III) oxide nanoparticles. Analytica Chimica Acta, 2013, 781, 48–53.

[94] Wang, H.; Hodgson, J.; Shrestha, T.B.; Thapa, P.S.; Moore, D.; Wu, X.; Ikenberry, M.; Troyer, D.L.; Wang, D.; Hohn, K.L.; Bossmann, S.H. Carbon dioxide hydrogenation to aromatic hydrocarbons. Beilstein J. Nanotechnol. 2014, 5, 760–769.

[95] Safari, J.; Zarnegar, Z. Sulphamic acid-functionalized magnetic Fe_3O_4 nanoparticles as recyclable catalyst for synthesis of imidazoles under microwave Irradiation. J. Chem. Sci. 2013, 125 (4), 835–841.

[96] Khodabakhshi, S.; Karami, B. Mojtaba Baghernejad Iron(II,III) oxide nanoparticle-catalyzed selective synthesis of unknown dihydropyrano[c]chromenes under green conditions. Monatsh Chem., 2014, 145, 1839–1843.

[97] Safari, J.; Zarnegar, Z. A magnetic nanoparticle-supported sulfuric acid as a highly efficient and reusable catalyst for rapid synthesis of amidoalkyl naphthols. Journal of Molecular Catalysis A: Chemical, 2013, 379, 269–276.

[98] Bayat, A.; Shakourian-Fard, M.; Ehyaei, N.; Mahmoodi Hashemi, M. Silver nanoparticles supported on silica-coated ferrite as magnetic and reusable catalysts for oxidant-free alcohol dehydrogenation. RSC Adv., 2015, 5, 22503–22509.

[99] Girija, G.; Bhojya Naik, H.S.; Vinay Kumar, B.; Sudhamani, C.N.; Harish, K.N. Fe_3O_4 nanoparticle supported Ni(II) complexes: A magnetically recoverable catalyst for Biginelli reaction. Arabian Journal of Chemistry, 2014, Available from: http://www.sciencedirect.com/science/article/pii/S1878535214001701, In press.

[100] Goodarz Naseri, M.; Saion, E.B.; Abbastabar Ahangar, H.; Halim Shaari, A.; Hashim, M. Simple Synthesis and Characterization of Cobalt Ferrite Nanoparticles by a Thermal Treatment Method. J. Nanomater. Volume 2010, Article ID 907686, 8 pp.

[101] Kaur Rajput, J.; Kaur, G. $CoFe_2O_4$ nanoparticles: An efficient heterogeneous magnetically separable catalyst for "click" synthesis of arylidene barbituric acid derivatives at room temperature. Chinese Journal of Catalysis, 2013, 34, 1697–1704.

[102] Kooti, M.; Afshari, M. Magnetic cobalt ferrite nanoparticles as an efficient catalyst for oxidation of alkenes. Scientia Iranica F, 2012, 19 (6), 1991–1995.

[103] Kamal Senapati, K.; Phukan, P. Magnetically separable cobalt ferrite nanocatalyst for aldol condensations of aldehydes and ketones. Bulletin of the Catalysis Society of India, 2011, 9, 1–8.

[104] Kumar, P.V.; Short, M.P.; Yip, S.; Yildiz, B.; Grossman, J.C. High Surface Reactivity and Water Adsorption on $NiFe_2O_4$ (111) Surfaces. J. Phys. Chem. C., 2013, 117 (11), 5678–5683.

[105] Hong, D.; Yamada, Y.; Nagatomi, T.; Takai, Y.; Fukuzumi, S.Catalysis of Nickel Ferrite for Photocatalytic Water Oxidation Using $[Ru(bpy)_3]^{2+}$ and $S_2O_8^{2-}$. J. Am. Chem. Soc. 2012, 134, 19572−19575.

[106] Radhakrishnan Nair, T.D.; Aniz, C.U. Effect of Redox Nature of Impregnated Ferrite Catalysts on Their Carbon Monoxide Oxidation Activity. RRJMS, 2013, 1 (2), 45–52.

[107] Wan, Q.; Li, P.; Shan, J.; Zhai, F.; Li, Z.; Qu, Z. Superior Catalytic Effect of Nickel Ferrite Nanoparticles in Improving Hydrogen Storage Properties of MgH_2. J. Phys. Chem. C, 2015, 119, 2925−2934.

[108] Eshghi, H.; Javid, A.; Khojastehnezhad, A.; Moeinpour, F.; Bamoharram, F.F.; Bakavoli, M.; Mirzaei, M. Preyssler heteropolyacid supported on silica coated $NiFe_2O_4$ nanoparticles for the catalytic synthesis of bis(dihydropyrimidinone)benzene and 3,4-dihydropyrimidin-2(1H)-ones. Chinese Journal of Catalysis, 2015, 36, 299–307.

[109] Lou, J.-C.; Chang, C.-K. Catalytic Oxidation of CO Over a Catalyst Produced in the Ferrite Process. Env. Eng. Sci., 2006, 23 (6), 1024–1032.

[110] Kasi Viswanath, I.V.; Murthy, Y. L. N. One-Pot, Three-Component Synthesis of 1, 4-Dihydropyridines by Using Nano Crystalline Copper Ferrite. Chem. Sci. Trans., 2013, 2 (1), 227–233.

[111] Murthy, Y. L. N.; Diwakar, B.S.; Govindh, B.; Nagalakshmi, K.; Kasi Viswanath, I.V.; Singh, R. Nano copper ferrite: A reusable catalyst for the synthesis of β,γ-unsaturated ketones. J. Chem. Sci., 2012,124 (3), 639–645.

[112] Gharib, A.; Noroozi Pesyan, N.; Vojdani Fard, L.; Roshani, M. Catalytic Synthesis of α-Aminonitriles Using Nano Copper Ferrite ($CuFe_2O_4$) under Green Conditions. Organic Chemistry International, Volume 2014, Article ID 169803, 8 pp.

[113] Yang, D.; Zhu, X.; Wei, W.; Jiang, M.; Zhang, N.; Ren, D.; You, J.; Wang, H. Magnetic Copper Ferrite Nanoparticles: An Inexpensive, Efficient, Recyclable Catalyst for the Synthesis of Substituted Benzoxazoles via Ullmann-Type Coupling under Ligand-Free Conditions. Synlett, 2014, 25, 729–735.

[114] Rashad, M.M.; Mohamed, R.M.; Ibrahim, M.A.; Ismail, L.F.M.; Abdel-Aal, E.A. Magnetic and catalytic properties of cubic copper ferrite nanopowders synthesized from secondary resources. Advanced Powder Technology, 2012, 23, 315–323.

[115] Papa, F.; Patron, L.; Carp, O.; Paraschiv, C.; Balint, I. Catalytic behavior of neodymium substituted zinc ferrites in oxidative coupling of methane. Rev. Roum. Chim. 2010, 55 (1), 33–38.

[116] Jadhav S.V.; Mohan Jinka, K.; Bajaj, H.C. Nanosized sulfated zinc ferrite as catalyst for the synthesis of nopol and other fine chemicals. Catalysis Today, 2012, 198, 98–105.

[117] de Moura, E.M.; Garcia, M.A.S.; Gonçalves, R.V.; Kiyohara, P.K.; Jardimc, R.F.; Rossi, L.M. Gold nanoparticles supported on magnesium ferrite and magnesium oxide for the selective oxidation of benzyl alcohol. RSC Adv., 2015, 5, 15035–15041.

[118] Han, A.; Liao, J.; Ye, M.; Yan, L.; Peng, X. Preparation of Nano-$MnFe_2O_4$ and Its Catalytic Performance of Thermal Decomposition of Ammonium Perchlorate. Chinese Journal of Chemical Engineering, 2011, 19(6), 1047–1051.

[119] Ghahremanzadeh, R.; Rashid, Z.; Zarnanic, A.-H.; Naeimi, H. Manganese ferrite nanoparticle catalyzed tandem and green synthesis of spirooxindoles. RSC Adv., 2014, 4, 43661–43670.

[120] Zhenyu, L.; Guangliang, X.; Yalin, Z. Microwave assisted low temperature synthesis of MnZn ferrite nanoparticles. Nanoscale Res. Lett. 2007, 2, 40–43.

[121] Velinov, N.; Koleva, K.; Tsoncheva, T.; Paneva, D.; Manova, E.; Kunev, B.; Mitov, I. Copper-cobalt ferrites as catalysts for methanol decomposition. 11th European Congress on Catalysis – EuropaCat-XI, Lyon, France, September 1st-6th, 2013.

[122] Wang, L.L.; He, H.Y. Surface Alkaline-Acidic Characteristics and Photo catalytic Properties of $Co_{1-x}Zn_xFe_2O_4$ Nano-particles Synthesized by Hydrothermal Method. J. Sci. Res. & Reports, 2014, 3 (2), 263–274; Article no. JSRR.2014.001.

[123] Khojastehnezhad, A.; Rahimizadeh, M.; Eshghi, H.; Moeinpour, F.; Bakavoli, M. Ferric hydrogen sulfate supported on silica-coated nickel ferrite nanoparticles as new and green magnetically separable catalyst for 1,8-dioxodecahydroacridine synthesis. Chinese J. Cat., 2014, 35, 376–382.

[124] Kumar B. Gupta, S.; Venkatachalam, A. Synthesis and characterization of spinel ferrites $Cu_{1-x}Cd_x[Fe_{1-x}Al_xCr_{1-x}Mn_x]O_4$. Rasayan J. Chem., 2010, 3 (4), 745–750.

[125] Dixit, R.; Gupta, P.; Saxena, R.; Dwivedi, R. Methylation of Aniline over Mn-Cu Ferrites Catalysts. Global Journal of Science Frontier Research Chemistry, 2013, 13 (7), 10 pp.

[126] Dandia, A.; Singh, R.; Joshi, J.; Maheshwari, S. Magnetically separable $CuFe_2O_4$ nanoparticles: an efficient catalyst for the synthesis of quinoxaline derivatives in tap-water under sonication. Eur. Chem. Bull., 2013, 2 (10), 825–829.

[127] Manova, E.; Estournès, C.; Paneva, D.; Reh, J.-L.; Tsoncheva, T.; Kunev, B.; Mitov, I. Mössbauer study of nanodimensional nickel ferrite – mechanochemical synthesis and catalytic properties. ICAME 2005 (Proceedings of the 28th International Conference on the Applications of the Mössbauer Effect (ICAME 2005), Montpellier, France, 4–9 September 2005, Volume I (Part I–II/V). Editors: Lippens, P.-E.; Jumas, J.-C.; Génin, J.-M. R.), 2007, 215–220.

[128] Wu, Y.; Song, M.; Xin, Z.; Zhang, X.; Zhang, Y.; Wang, C.; Li, S.; Gu, N. Ultra-small particles of iron oxide as peroxidase for immunohistochemical detection. Nanotech., 2011, 22, 225703, 8 pp.